Remote Sensing Applications: Society and Environment 41 (2026) 101868

Contents lists available at ScienceDirect

Remote Sensing Applications: Society and Environment

journal homepage: www.elsevier.com/locate/rsase

Validation of Himawari-8/9 10-minute wildfire products: Comparisons with MODIS and VIIRS from 2015 to 2023

Zifeng Liu, Qiang Zhang *, Baomo Zhang, Jian Zhu

Information Science and Technology College, Dalian Maritime University, Dalian, China

ARTICLE INFO

Keywords:
Wildfire
Himawari-8/9
Validation
MODIS
VIIRS

ABSTRACT

In recent years, wildfires have occurred frequently around the world, which not only greatly threaten the social security, but also cause serious pollution to the environment. Currently, remote sensing satellites can monitor wildfires with a large range and long time-series data. These satellites can be divided into two types: geostationary satellites (such as Himawari-8/9) and polar-orbiting satellites (such as MODIS/VIIRS). In this paper, MODIS and VIIRS polar-orbiting satellite wildfire products from 2015 to 2022 are used as the comparative data, to verify the accuracy and effectiveness of Himawari-8/9 10-minute near real-time wildfire products. Firstly, we utilize the polar orbit satellite data to analyze the wildfire detection accuracy as well as the fire radiative power (FRP) estimation ability for Himawari-8/9. Secondly, we compare the new (Himawari-9) with old (Himawari-8) satellite sensors on wildfire detection ability. The results show that, due to the advantage of high temporal resolution, Himawari-8/9 wildfire products have more fire hotspot numbers in the same range than MODIS and VIIRS. Due to the insufficient spatial resolution at 2-km level, the omission rate of Himawari-8/9 wildfire products comparison with VIIRS is higher than that of comparison with MODIS. Especially in spring and summer, there is a peak period of Himawari-8/9 omission rate. For large wildfires, Himawari-8/9 wildfire products show a lower omission rate and stronger detection capability. However, in terms of FRP retrieval, due to the difference in spatial resolution of different sensors, the Himawari-8/9 wildfire products contrastive with MODIS show a smaller difference than its contrastive with VIIRS. In addition, Himawari-9 unexpectedly shows slightly weaker fire hotspot detection capability than Himawari-8. Finally, based on above validation works, this paper provides the more effective algorithm design idea, for the near real-time wildfire detection of geostationary satellites.

1. Introduction

Wildfires are greatly harmful to human society and environment (Moritz et al., 2014; Wang et al., 2024). Therefore, real-time monitoring and control of wildfire is crucial and indispensable (Tymstra et al., 2020). However, due to the temporal and spatial randomness of wildfires, how to effectively and timely detect wildfires become a huge challenge (Bowman et al., 2017).

Current ground monitoring ways for wildfire include three types (Mohapatra and Trinh, 2022; Touge et al., 2024): manual inspection, ground sensor network, and unmanned aerial vehicle (UAV). For instance, forest inspectors are organized to conduct manual inspection in special areas with high fire risk. Obviously, this way consumes a lot of manpower and resources. Moreover, it is difficult to monitor the fire in the rugged regions (Tedim et al., 2018). In addition, assigning the fire sensor networks on the

* Corresponding author.
E-mail address: qzhang95@dlmu.edu.cn (Q. Zhang).

https://doi.org/10.1016/j.rsase.2026.101868
Received 26 July 2025; Received in revised form 23 December 2025; Accepted 1 January 2026
Available online 2 January 2026

ground could also detect the occurrence of fire (Aslan et al., 2012). However, this way pays the high economic cost and is easy to be damaged. At the same time, it also requires a lot of manpower in the initial deployment process of sensors, especially in the faraway areas. In recent years, UAV inspection is also a common way of monitoring fire. The UAV is equipped with an optical camera or a thermal infrared imager, to perform flight monitoring in appointed areas. However, due to power and signal distance limitations, the flight time of UAV is usually short (Cruz et al., 2016). Generally, the above ground monitoring methods are exposed to various types of shortcomings and limitations, which are not conducive to the timely detection and control of wildfires (Mohapatra and Trinh, 2022).

Compared with the ground monitoring, remote sensing satellites could realize the wildfire monitoring in a large-range, long time-series and low-cost way (Zhang et al., 2022b). Currently, there are two types of satellite for fire monitoring: polar-orbiting satellites and geostationary satellites (Coppo, 2015; Chen et al., 2022).

Polar orbit satellites could achieve high spatial resolution, and monitor the ground with global scale (Zhang et al., 2024b,a). Such as Aqua and Terra satellites with Moderate Resolution Imaging Spectroradiometer (MODIS) sensor, Suomi National Polar-Orbiting Partnership (NPP) satellites with Visible Infrared Imaging Radiometer Suite (VIIRS) sensor, and Sentinel-3 satellites with Sea Land Surface Temperature Radiometer (SLSTR) sensor. Whereas polar orbit satellites usually own the low temporal resolution, which require more than ten hours or several days to observe again for the same regions. Therefore, the wildfire detection accuracy of polar-orbiting satellites is usually high, while it cannot achieve the near real-time fire monitoring (Chatzopoulos-Vouzoglanis et al., 2023; Hantson et al., 2013).

In contrast, geostationary satellites have high temporal resolution, which could reach 10 min or even a few minutes, while their spatial resolution is low and cannot achieve global monitoring. Such as National Oceanic and Atmospheric Administration (NOAA)'s Geostationary Operational Environmental Satellite (GOES) series, the European Organization for the Exploitation of Meteorological Satellites (EUMETSAT), Meteosat Second Generation (MSG) satellites, China's Fengyun-4 series satellites, and Japan Aerospace Exploration Agency's (JAXA) Himawari-8/9 satellites. Geostationary satellites could realize the near real-time monitoring of wildfires (Chen et al., 2023; Li et al., 2020). Nevertheless, the fire detection accuracy of geostationary satellites is usually low because of the low spatial resolution.

Compared with the polar orbit satellites, the spatial resolution of the geostationary satellites is coarser. However, the advantage of their high temporal resolution makes them realize continuous, fast and near real-time wildfire monitoring. This is critical for early wildfire detection. Therefore, although previous studies on remote sensing fire monitoring preferred polar-orbiting satellites (Justice et al., 2002; Giglio et al., 2016). Generally, in recent years, there are more and more researches on wildfire using geostationary satellite, which has gradually become a hot field (Zhang et al., 2023).

Himawari-8/9 are the new generation of geostationary meteorological satellite launched by JAXA. They conduct monitoring (East Asia, Southeast Asia and Oceania) at every 10 min in the full disk regions. Through the threshold algorithm, JAXA generates the level-2 2-km spatial resolution and 10 min near real-time wildfire products (Chen et al., 2023). Due to the low spatial resolution of Himawari-8/9 satellites, the accuracy and reliability of these level-2 wildfire products still need to be verified. In contrast, polar-orbiting satellites have higher spatial resolution. Hence, their wildfire detection accuracy is usually higher than geostationary satellites. Therefore, the wildfire products of the polar-orbiting satellites (MODIS and VIIRS) could be utilized as the reference data, to verify the accuracy and effectiveness of the Himawari-8/9 satellites level-2 wildfire products in the full disk regions.

In recent years, some studies have focused on the validation of Himawari series fire products. Wickramasinghe et al. (2020) focused on the AHI-FSA fire hotspots monitoring algorithm of Himawari-8. It relied on MODIS, VIIRS polar-orbiting satellite products and Landsat-8 burn area data. Targeted validation was conducted during the dry season in northern Australia in 2016. However, the 10-minute high-frequency data of AHI-FSA was aggregated into hourly composite products. These products were compared with MODIS/VIIRS daily composite products to calculate omission errors. This aggregation lost the high-frequency monitoring advantage of AHI-FSA. Chen et al. (2022) compared the detection performance of different satellite fire products (MODIS, VIIRS, Himawari-8) in East China. It focused on verifying the recognition ability of small agricultural fires and short-duration fires. It revealed the impact of spatial/temporal resolution on detection results. However, the study had a short time span and small research area. It could hardly represent the validation needs of different climates and scenarios. Chatzopoulos-Vouzoglanis et al. (2023) took Australia's 2019–2020 period (including the "Black Summer" extreme wildfire season) as the research period. It focused on the BRIGHT/FRP products of Himawari-8 AHI. Comparative validation was carried out with MODIS (MOD14/MYD14) and VIIRS (VNP14IMG) polar-orbiting satellite fire products. Multi-dimensional validation showed that AHI's coarse spatial resolution led to omission of low-intensity fire hotspots. It also caused underestimation of FRP for high-intensity fire hotspots. However, the study was only based on single-year data from 2019 to 2020. It did not analyze the long-term stability of the product. It also lacked error quantification indicators.

In the past, validation studies based on Himawari series satellites had the following shortcomings. The validation time span was short. The spatial coverage was small. The validation method system was single. There was a lack of comparison between the new and old sensors of Himawari-8/9.

This study establishes a complete and systematic validation framework for Himawari-8/9 wildfire products. It features a long validation time span and wide validation scope. The verification work of this paper is divided into the three parts: Verification of the wildfire detection capability for Himawari-8 satellite; Verification of the FRP retrieval capability for Himawari-8 satellite; Comparison between the old sensor of Himawari-8 satellite and the new sensor of Himawari-9 satellite. The specific contributions are listed as follows:

- This work compares the wildfire products of Himawari-8 with MODIS and VIIRS on a long time-series scale from 2015 to 2022. We analyze the number of fire hotspots under different season, the fire frequency under different seasons, and the situation of satellite fire hotspots difference.

Table 1
The information of three satellite wildfire products for Himawari-8/9, MODIS and VIIRS.

Wildfire products	Temporal resolution	Spatial resolution	Spectral range (μm)
Himawari-8/9 Level-2	**10-minute**	2-km	0.47–13.3
MODIS	1-day	1-km	**0.40–14.4**
VIIRS	1-day	**375 m**	0.40–12.5

- This work discusses the similarities and differences of the fire hotspot distribution for Himawari-8 and MODIS/VIIRS wildfire products during 2020–2022, in Sichuan Province, China. From the perspective of land cover types, climate and human activities, the analysis of three satellites wildfire distribution is given.
- Based on MODIS and VIIRS wildfire products as the reference data and spatio-temporal matching under different conditions with Himawari-8 satellite from 2015 to 2022, we analyze the wildfire detection ability in different time, different seasons, different land cover types, and different FRP for Himawari-8 wildfire products.
- This work analyzes the fire hotspot FRP distribution of three satellites (Himawari-8, MODIS, VIIRS) during 2022, and discusses the consistency and differences in their FRP distribution and the reasons. In addition, under the three types of land cover (forest, farmland and shrub) with high fire incidence, we discuss the FRP retrieval capability of Himawari-8 with MODIS and VIIRS.
- Compared Himawari-8 wildfire products with Himawari-9 in October and November 2022, this work calculates the omission rate and consistency, to analyze the reasons for the differences via mutual spatio-temporal matching.
- Based on ground truth fire data collected through experts, drones and other methods, the ability of Himawari-8/9 wildfire products to detect real fires and their capability for near real-time fire detection are analyzed.

2. Data

This work uses multi-source remote sensing satellite data, to verify the accuracy and effectiveness of Himawari-8/9 JAXA level-2 2-km spatial resolution and 10 min near real-time wildfire products. The main wildfire products used are given below: Himawari-8/9 level-2 wildfire products, MODIS MCD14ML wildfire products, and VIIRS VNP14IMGML wildfire products. The information of three satellites wildfire products is shown in Table 1. In addition, we also utilize the CCI-LC land cover products as the auxiliary data. The details are described as follows.

2.1. Himawari-8/9 level-2 10-minute wildfire products

JAXA launched the new generation geostationary satellite Himawari-8 in October 2014, followed by Himawari-9 in November 2016 (Bessho et al., 2016). Two satellites carry the Advanced Himawari Imager (AHI) sensors with the same spatial resolution and temporal resolution. Compared with the previous generation geostationary satellites, Himawari-8/9 have greatly improved for earth observation (Bessho et al., 2016). Himawari-8 served as the primary observation satellite until 13 December 2022. Before December 13, 2022, a period about 2 months is the transition stage using both Himawari-8 and Himawari-9. After December 13, 2022, the handover time was completed, where Himawari-9 has served as the primary observation satellite up to now.

As shown in Fig. 1, in terms of the observation range, Himawari-8/9 satellites are mainly used for monitoring in East Asia, Southeast Asia and Australia. The full disk observation range of Himawari-8/9 distributes from 60° N to 60° S and 160° W to 80° E. For the temporal resolution, Himawari-8/9 observe the full disk regions at every 10 min. For the spectral distribution, AHI has a total of 16 bands, from visible to thermal infrared band. These bands range from 0.47 μm to 13.3 μm. In terms of the spatial resolution, the thermal infrared band is 2 km, and the visible band is 0.5/1/2 km.

For the wildfire products, JAXA uses the brightness temperature difference between the target pixel and its surrounding pixels to determine the fire hotspots (Zhang et al., 2025). It uses the AHI 7-th band (3.9 μm) and 14-th band (10.8 μm) to estimate the normalized deviation between the brightness temperature of the target pixel and the surrounding background pixels. Its algorithm employs the 6-th band (2.3 μm) and 7-th band (3.9 μm) via double spectrum method, to estimate the value of FRP. Double spectrum method calculates the fire temperature and determines the fire level of fire hotspot. The reliability of the fire hotspot is calculated by the angle of the sun and other factors.

Since March 2015, JAXA has generated and released the level-2 10-minute wildfire products, via CSV format file. The products contain near real-time fire hotspot, as well as the fire hotspot time, longitude, latitude, FRP and other key information. The delay time is about 30 min. This work uses Himawari-8/9 10-minute level-2 wildfire (WLF) products from April 2015 to December 2022. The products could be publicly downloaded from JAXA's website: https://www.eorc.jaxa.jp/ptree/.

2.2. MODIS MCD14ML wildfire products

MODIS sensor is both carried on Terra and Aqua satellites. The two polar-orbit satellites were respectively launched by National Aeronautics and Space Administration (NASA) in 1998 and 2002. The spatial resolution for wildfire detection in the thermal infrared band is 1 km. As a dual-star combined system, MODIS has a higher temporal resolution than a single-star sensor. It could monitor the same regions twice time within a day. MODIS sensor has 36 bands. Its spectral range starts from visible to thermal infrared band, whose wavelength range is fixed from 0.4 to 14.4 μm.

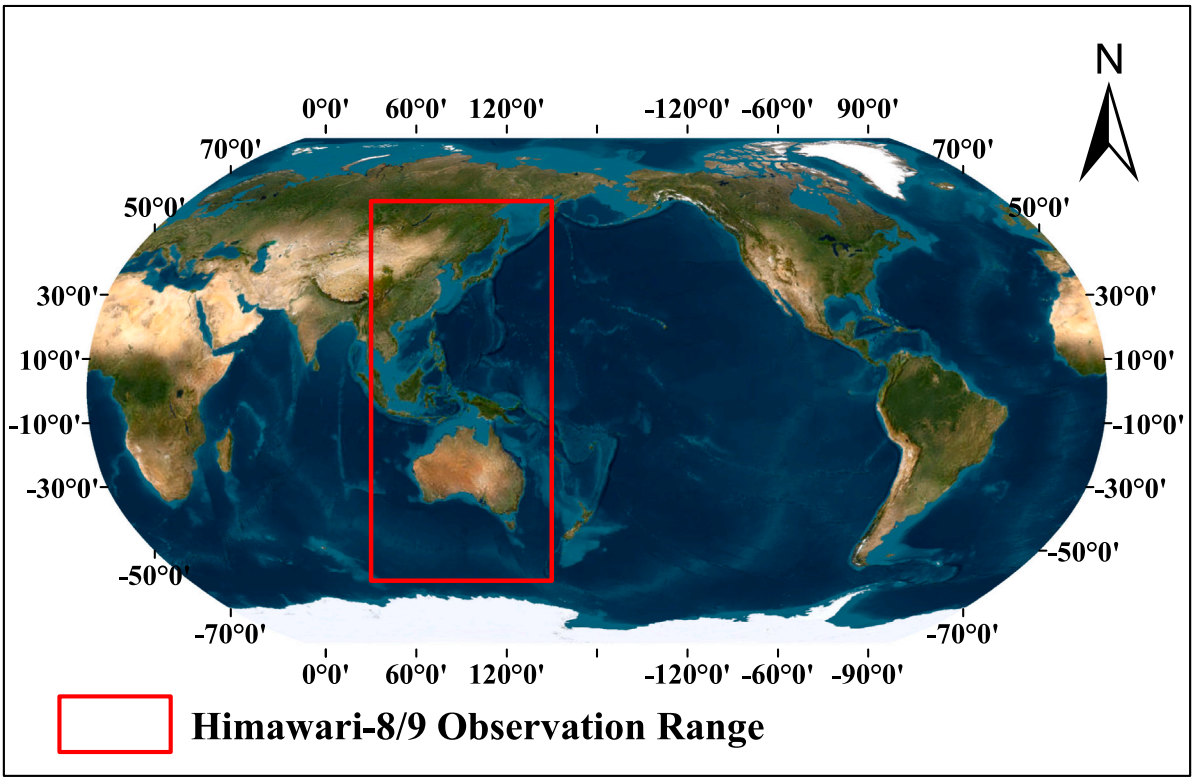

Fig. 1. The full disk observation range of Himawari-8/9 satellites.

MODIS Collection-6 wildfire products (MCD14ML) use context algorithm, to detect the fire hotspots in the global land (Giglio et al., 2021). This work uses the global data of MODIS products. Since 2000, these products could be downloaded from the University of Maryland's FTP website: fuoco.geog.umd.edu. The format of MCD14ML wildfire products is ASCII file, which includes the fire hotspot detected by MODIS within a month. It records the latitude and longitude of the fire hotspot, time, the types of fire, confidence, FRP and other information. In this work, we utilize the MODIS MCD14ML wildfire products from April 2015 to December 2022 as the auxiliary data. In order to verify and analyze the Himawari-8/9 wildfire products, this work selects the fire hotspots of the MODIS MCD14ML fire products, which are located at the Himawari-8/9 full disk regions in Fig. 1.

2.3. VIIRS VNP14IMGML wildfire products

VIIRS, a polar-orbiting satellite sensor like MODIS, was launched on the S-NPP satellite in 2011 and then on the NOAA-20 satellite in 2017. At the end of 2023, NOAA-21 carried VIIRS for land, ocean, and atmospheric monitoring tasks. VIIRS is also widely applied for fire detection. Compared with MODIS sensor, it has a spatial resolution of 375 m in the band used for fire detection, which is higher than MODIS (Wickramasinghe et al., 2020). Therefore, VIIRS has a stronger detection capability than MODIS for the small fires and fire hotspots around fire edge. The SNPP-VIIRS satellite crosses the equator at 1:30 p.m. and 1:30 a.m every day. VIIRS has 22 spectral bands, including visible, short-wave infrared, mid-infrared, thermal infrared and other bands from 0.4 to 12.5 μm.

VIIRS Collection-1 and Collection-2 wildfire products (VNP14IMGML) detect the fire hotspots using a contextual algorithm, which is similar to MODIS wildfire products (Schroeder and Giglio, 2018; Schroeder et al., 2024). This work uses VIIRS VNP14IMGML wildfire products as the auxiliary data. VIIRS VNP14IMGML wildfire products also contain the latitude and longitude of the detected points, occurrence time, type of fire, confidence, FRP and other key information every month. We downloaded the VNP14IMGML Collection-1 wildfire products from April 2015 to August 2022. Since these products were only updated to August 2022, the VNP14IMGML Collection-2 wildfire products from September 2022 to December 2022 were downloaded and employed in this work. Similar with the MODIS MCD14ML wildfire products, this work selects the fire hotspots of VIIRS VNP14IMGML wildfire products within the Himawari-8/9 full disk regions. VIIRS VNP14IMGML wildfire products are available by FTP downloading from the University of Maryland's website at: fuoco.geog.umd.edu.

2.4. ESA CCI land cover products

European Space Agency (ESA) Climate Change Initiative (CCI) land cover products are the global land cover data with a spatial resolution of 300 m (CCI, ESA Land Cover, 2017). These ESA CCI land cover products are updated once a year. This work downloads

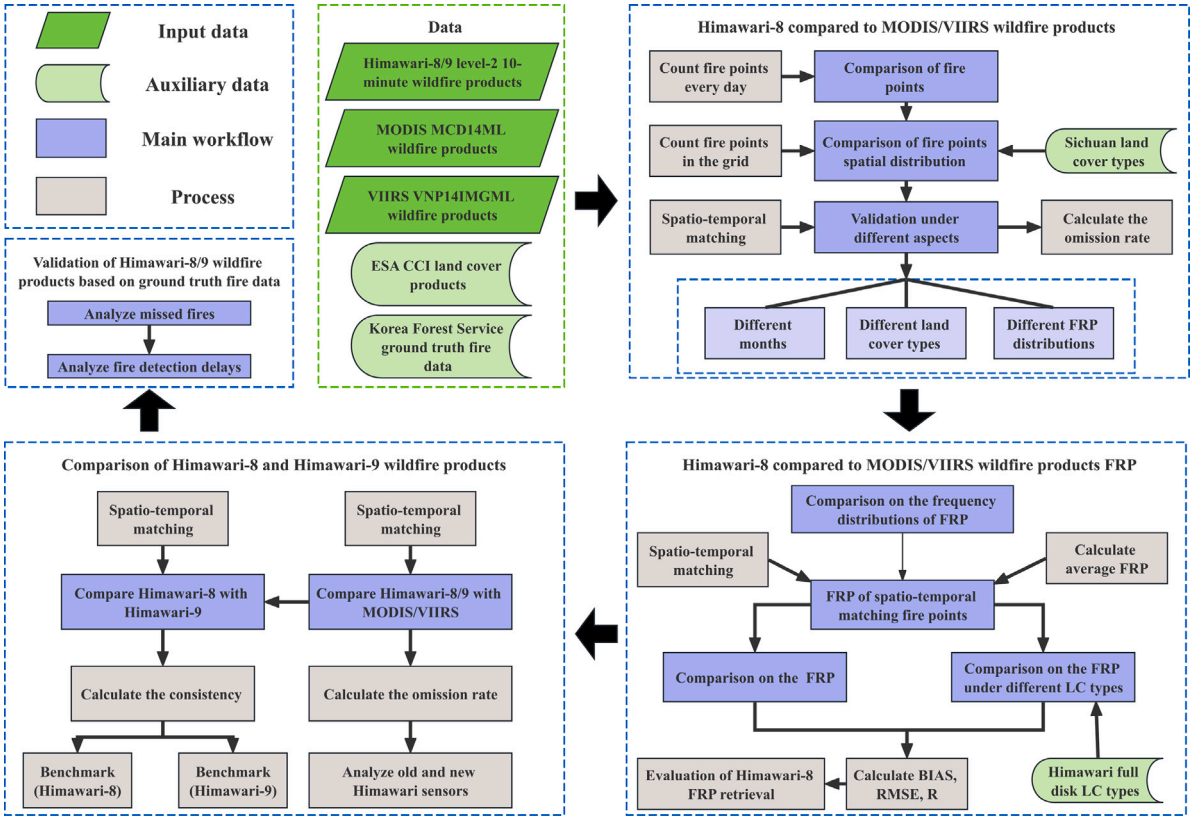

Fig. 2. Flowchart of the overall work for the validation of Himawari-8/9 wildfire products.

the ESA CCI LC-V2 products from 2015 to 2022. According to the land cover types given by these products, the land cover types within Himawari-8/9 full disk regions are divided into: Agriculture, forest, grassland, wetland, shrubland, sparse vegetation, bare area, and water. The ESA CCI land cover products could be downloaded at: https://maps.elie.ucl.ac.be/CCI/viewer/download.php.

2.5. Ground truth fire data

The Korea Forest Service provides ground truth fire data for South Korea, collected through experts, drones and other methods. The data includes the start time, end time, location and damaged area of the fires. This study selects 70 fire incidents from 2022 to 2023, including 12 fires with damaged areas less than 10 and 58 fires with damaged areas of 10 ha or more. The potential of Himawari satellites for real fire detection is validated using these 70 real fire incidents. The ground truth fire data could be downloaded from the official website of the Korea Forest Service: https://www.forest.go.kr.

3. Verification method and results

The flowchart for the validation of Himawari-8/9 wildfire products is shown in Fig. 2. The overall verification work is divided into four parts. The first part is Himawari-8 wildfire products comparison with MODIS and VIIRS wildfire products, which corresponds to Sections 3.1 and 3.2. The second part is comparison FRP of Himawari-8 wildfire products with MODIS/VIIRS, which corresponds to Sections 3.2.4–3.2.6 . The third part is comparison of the new and old satellites Himawari-8 and Himawari-9 wildfire products, which corresponds to Section 3.3. The last part is validation of Himawari-8/9 wildfire products based on ground truth fire data, which corresponds to Section 3.4.

3.1. Statistical indicator

The omission rate of wildfire products is an important indicator (Bastarrika et al., 2011), which represents the proportion of missing fire hotspots over a period of time. In addition, the consistency between wildfire products is a similarity indicator, which represents the proportion of fire hotspots both detected by two wildfire products over a period of time.

In this work, the omission rate refers to the proportion of the fire hotspots missed by the geostationary satellite with polar-orbiting satellite. It uses the polar-orbiting satellite wildfire products as the benchmark data, to verify the geostationary satellite fire products.

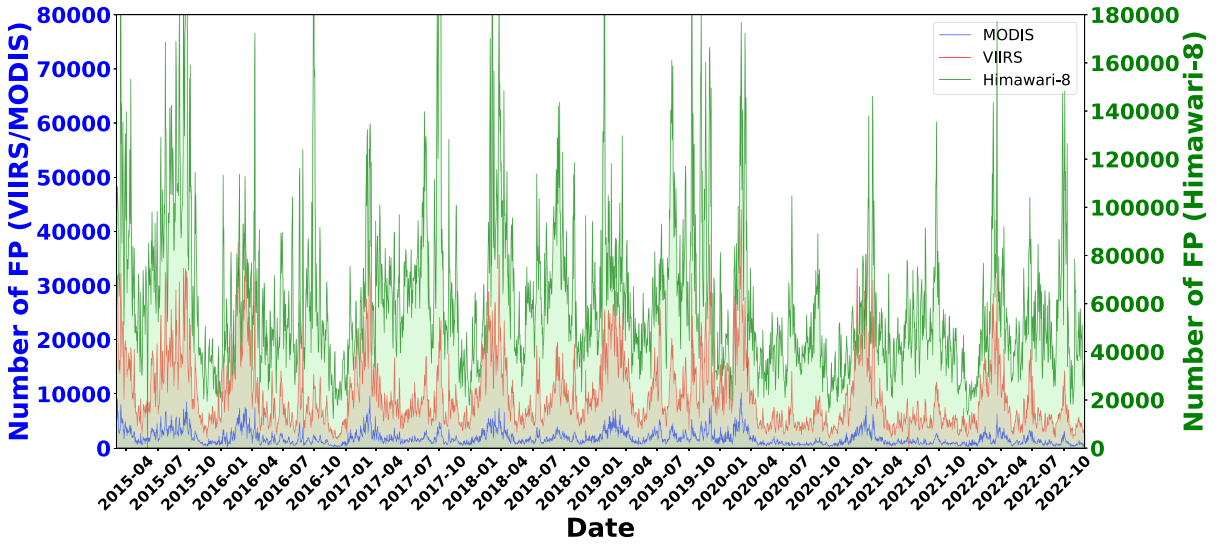

Fig. 3. Daily number of fire hotspots in the three satellite wildfire products from April 2015 to December 2022 (Left is VIIRS and MODIS; Right is Himawari-8).

The omission rate is calculated below:

$$\mathbf{Oms} = 1 - \frac{\mathbf{M}}{\mathbf{T}} \tag{1}$$

where **Oms** is the omission rate of geostationary satellites Himawari-8/9 wildfire products, compared with polar-orbiting satellites MODIS/VIIRS wildfire products. **M** denotes the number of fire hotspots successfully matched between the benchmark wildfire products and the target wildfire products. **T** refers to the total number of all fire hotspots in target wildfire products.

In terms of the consistency indicator, when the spatio-temporal matching between two satellites wildfire products, it represents the proportion of the fire hotspots detected by the geostationary satellite with polar-orbiting satellite. The consistency indicator is calculated below:

$$\mathbf{Con} = \frac{\mathbf{M}}{\mathbf{T}} \tag{2}$$

where **Con** stands for the consistency between two satellite wildfire products.

3.2. Compared Himawari-8 wildfire products with MODIS and VIIRS wildfire products

3.2.1. Comparisons on the number of fire hotspots

Firstly, this work statistics the daily number of fire hotspots for MODIS, VIIRS, Himawari-8 wildfire products from April 2015 to December 2022. It is important to note that the fire hotspots of MODIS and VIIRS wildfire products do not include fires around the world, which just select the fire hotspots within the Himawari-8 full disk regions. For the fire hotspots of Himawari-8 wildfire products, this work only adopts the fire hotspots before and after 10 min corresponding to the observed time points of MODIS and VIIRS wildfire products. It is conducive to analyze the trend of fire number change of three satellite wildfire products in the same time and in the same regions.

In addition, this work also statistics the average monthly number of fire hotspots for Himawari-8, MODIS and VIIRS wildfire products. Through these statistical data, the difference and consistency for the number of fire hotspots could be indirectly analyzed via the frequency and change rule in these three long time-series wildfire products.

Fig. 3 depicts the daily number of fire hotspots in the three satellite wildfire products from April 2015 to December 2022. Obviously, the daily number of fire hotspots in Himawari-8 wildfire products is more than that of MODIS and VIIRS wildfire products. Because of the high temporal resolution for geostationary satellites, Himawari-8 could observe the full disk regions at every 10 min. However, MODIS and VIIRS could continuously observe the same regions at only every day (Tang et al., 2020). It allows Himawari-8 to detect much more fire hotspots than MODIS and VIIRS. This also reflects the advantage of high temporal resolution for geostationary satellites, which could perform high-frequency observation of fires at minute level (Zhang et al., 2022a).

Compared the daily number of fire hotspots for MODIS with VIIRS wildfire products in Fig. 3, the average daily number of fire hotspots for VIIRS wildfire products is higher than that of MODIS wildfire products. The main reason is that the difference for the spatial resolution of the two sensors (Schroeder et al., 2014). VIIRS VNP14IMGML products have the spatial resolution of 375 m, whereas MODIS MCD14ML products have the spatial resolution of 1 km. It indicates that the area of a MODIS pixel is much larger than that of VIIRS. For small fires, such as agricultural fires or fire hotspots around the edge of central fire, they usually behave

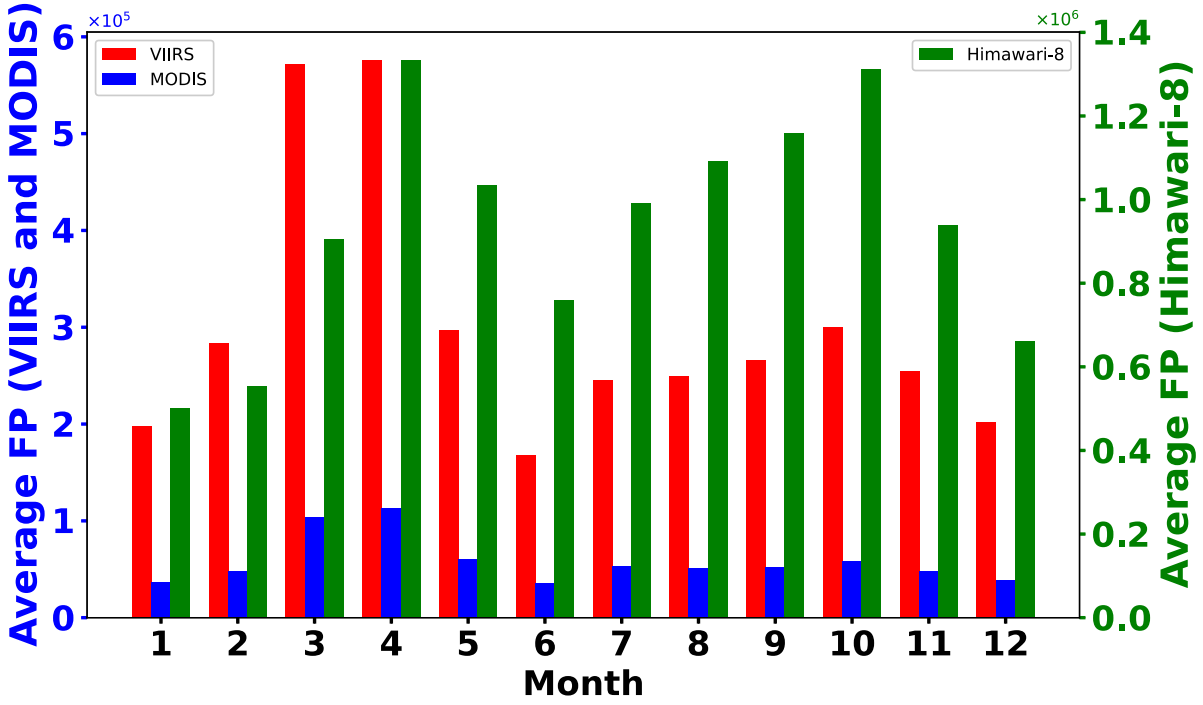

Fig. 4. Average monthly number of fire hotspots in the three satellite wildfire products from April 2015 to December 2022 (Left is VIIRS and MODIS; Right is Himawari-8).

smaller in MODIS than VIIRS. Therefore, it is easier for MODIS to miss these fire hotspots. In contrast, VIIRS has a better performance for detection of small fire hotspots (Fu et al., 2020)

From the consistency for the number of fire hotspots in the three wildfire products in Fig. 3, MODIS, VIIRS and Himawari-8 wildfire products show a similar consistency. Their numbers of fire hotspots have the homogeneous change in the long time-series products. Although the change in the number of fire hotspots is different, it is similar in terms of the trend of change. This phenomenon is mainly due to the three satellite wildfire products using the context algorithm. This algorithm employs the difference between the brightness temperature of the target pixel and the background pixel to detect the fire hotspots (Giglio et al., 2003). Although Himawari-8 is a geostationary satellite, JAXA does not use the temporal information for level-2 10-minute wildfire products. In Fig. 3, the number of fire hotspots on some dates is 0. It is not that no fire hotspot is detected at that day. The reason is satellite sensor at that day is maintained. As a result, fire hotspot is not effectively detected at that day.

Fig. 4 shows the average monthly number of fire hotspots in the three satellite wildfire products from April 2015 to December 2022. The three wildfire products have high similarity in the rise and fall of fire hotspots in different months. They all perform the first peak in March, April, and May. And their second peak occur in September, October, and November. MODIS, VIIRS, and Himawari-8 wildfire products all behave the highest number of average monthly fire hotspots in April, with 112 814 points in MODIS wildfire products, 576 162 points in VIIRS wildfire products, and 1 334 120 points in Himawari-8 wildfire products. For the lowest number of average monthly fire hotspots, MODIS and VIIRS wildfire products appear in June, whose points are 36 079 for MODIS wildfire products, 168 100 for VIIRS wildfire products, respectively. Himawari-8 wildfire products appear in January with a fire hotspot of 501 258. The main reason is that March, April and May are spring in the Northern Hemisphere. The land surface temperature begins to warm and plants flourish in this period. Therefore, the amount of fuel increases and wildfire becomes more frequent in March, April and May.

In contrast, March, April and May in the Southern Hemisphere are autumn. The weather is usually dry in this period. Leaves are mostly piled on the ground, providing the more favorable conditions for the burning and spreading of wildfire (Mitchell, 2023). In addition, spring and autumn are the two most frequent seasons for straw burning (Cui et al., 2021), which also increases the probability of wildfire. In conclusion, wildfires are frequent in March, April and May, which also causes the first peak fire of Himawari-8 wildfire products. The opposite is that in September, October, and November, when the northern Hemisphere is in autumn and the southern Hemisphere is in Spring. This stage is also a high wildfire incidence period, which leads to the second fire peak of Himawari-8 wildfire products.

3.2.2. Comparisons on the spatial distribution

In order to better analyze the spatial distribution difference and consistency between Himawari-8 and MODIS, VIIRS wildfire products, this work selects the period 2020–2022 in China's Sichuan Province as the comparative regions. In this paper, the selected

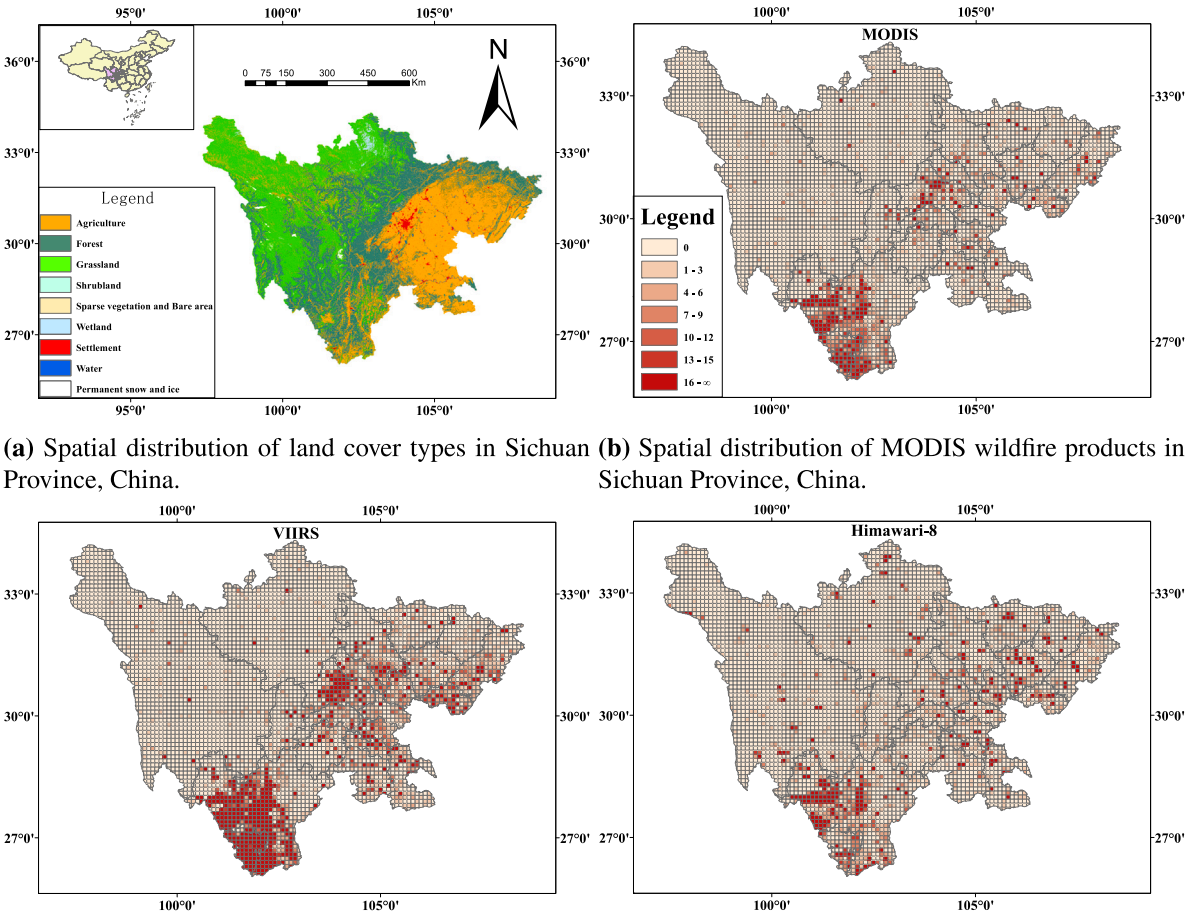

(a) Spatial distribution of land cover types in Sichuan Province, China.

(b) Spatial distribution of MODIS wildfire products in Sichuan Province, China.

(c) Spatial distribution of VIIRS wildfire products in Sichuan Province, China.

(d) Spatial distribution of Himawari-8 wildfire products in Sichuan Province, China.

Fig. 5. The land cover type and spatial distribution of MODIS, VIIRS and Himawari-8 wildfire products in Sichuan Province, China from 2020 to 2022. For panels (b)–(d), the fire point distribution is visualized based on a 0.1° × 0.1° latitude and longitude grid, with different colors representing the number of fire points in each grid to highlight the aggregation characteristics of fire points.

regions is divided into 0.1° × 0.1° latitude and longitude grid and the number of fire hotspots on each grid is counted for Himawari-8 and MODIS/VIIRS. In addition, according to the number of fire hotspots, each grid is behaved with different color. Based on this strategy, we could more effectively distinguish the gathering fire hotspots.

The spatial distribution of fire hotspots and land cover types of the three satellite wildfire products in Sichuan Province during 2020–2022 are shown in Fig. 5. Figs. 5(b)–5(c) are the fire hotspot distribution of MODIS and VIIRS wildfire products, respectively. The spatial distribution of fire hotspots between the two wildfire products behaves a high consistency. Most of the fire hotspots are concentrated in the southern regions of Sichuan, while some points are concentrated in the eastern regions of the province and around the city of Chengdu. The concentration of fire hotspots in VIIRS wildfire products is more obvious than that of MODIS wildfire products. There are only a few scattered fire hotspots in other areas. Himawari-8 wildfire products also behave a large concentration of fire hotspots in the southern regions of Sichuan Province. Whereas it is different from MODIS and VIIRS wildfire products. Without obvious fire hotspots focused around the urban regions of Chengdu, the fire hotspots appear relatively scattered in Fig. 5(d).

According to the land cover type of Sichuan Province in Fig. 5(a), there are a large number of forests, farmland and grasslands in the southern regions of Sichuan Province. The main vegetation types are evergreen broad-leaved forest (Zhao et al., 2014), whose flammability is high. Most terrain is mountains and hills, which is more conducive to the rapid spread of fire (Sharples, 2009). In terms of climate, the region has distinct dry and wet seasons, especially in spring and autumn. This provides more favorable conditions for the occurrence of fires (Swaine, 1992). In addition, in the southern regions of Sichuan Province, human farming activities are more frequent (Zheng et al., 2012). Therefore, agricultural fires occur more frequently in these regions. In the eastern regions of Sichuan Province, which are mostly farmland, there are part fire hotspots caused by agricultural activities. In the urban regions of Chengdu, the concentrated fire hotspots are mostly false fire hotspots. The main reason may be that there are a large

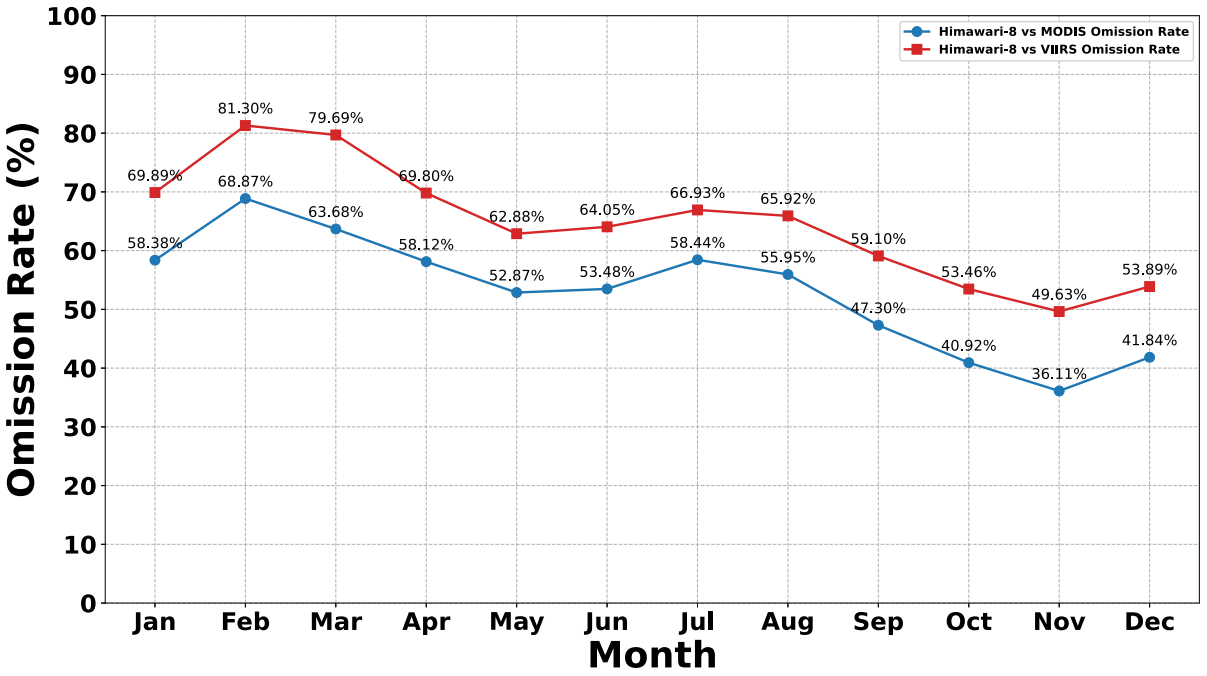

Fig. 6. The omission rate of Himawari-8 wildfire products, under different months according to the spatio-temporal matching of MODIS and VIIRS wildfire products.

number of high-temperature factories in urban regions. These factories are mistakenly detected as the fire hotspots.

As portrayed in Fig. 5, the fire hotspots of MODIS and VIIRS wildfire products appear to be more concentrated, while the fire hotspots of Himawari-8 wildfire products are more dispersed. Although the observation frequency of Himawari-8 is higher than MODIS and VIIRS. However, due to the limitations in spatial resolution, it is difficult for Himawari-8 to detect small fires, resulting in more dispersed fire hotspots. The spatial distribution of fire hotspots of the MODIS and VIIRS wildfire products reflects a high similarity, while Himawari-8 wildfire products show a low similarity with them. The main reason is that MODIS and VIIRS sensors have strong homogeneity, and their wildfire detection algorithms are also similar (Justice et al., 2002; Schroeder et al., 2014). However, there are still some differences between Himawari-8 and MODIS and VIIRS in both sensor and algorithm designing, which result in the low consistency of spatial distribution for fire hotspots.

3.2.3. Comparisons on the different months/land cover/FRP distribution

In this section, the fire hotspots of MODIS, VIIRS and Himawari-8 wildfire products are temporal-spatial matched. The MODIS and VIIRS wildfire products during April 2015 to December 2022 are selected as the analysis objects, to calculate the omission rate of Himawari-8 wildfire products. Considering the differences of temporal resolution and spatial resolution for the three satellite wildfire products, the temporal-spatial matching rule is determined as follows.

For MODIS and VIIRS fire hotspots, the haversine distance of spatial range is lower than 2.5 km. Before and after the fire hotspot within 30 min, if there is at least one Himawari-8 fire hotspot, the temporal-spatial matching of this fire hotspot is successful. Otherwise, it is considered that this fire hotspot cannot be matched with the Himawari-8 wildfire products.

Then from the perspective of different months, land cover types and FRP distribution, we verify and analyze Himawari-8 wildfire products: (a) For different months, referring to analyze the fire hotspot detection ability of Himawari-8 wildfire products in different time intervals; (b) For different land cover types, referring to the analysis of Himawari-8 wildfire detection accuracy in combustible and non-combustible substances; (c) For different FRP distribution, referring to analyze the reliability of Himawari-8 wildfire detection under different fire sizes.

(a) Verifying and analyzing Himawari-8 wildfire products under different months

As shown in Fig. 6, this work verifies the omission rate of Himawari-8 fire products, under different months according to the temporal-spatial matching of MODIS and VIIRS wildfire products. The monthly omission rate of Himawari-8 versus MODIS wildfire products is about 10%, which is lower than that of Himawari-8 versus VIIRS wildfire products. The month with the largest difference is March, with a difference of 16.01%. The month with the smallest difference is July, with a difference of 8.49%.

The main reason for this situation is the spatial resolution difference between the two polar-orbiting satellite sensors. Small fires are usually difficult to detect, which is the limitation of most remote sensing satellites (Mohapatra and Trinh, 2022). The spatial resolution of Himawari-8 wildfire products is 2 km, while the spatial resolution of MODIS wildfire products is 1 km. The

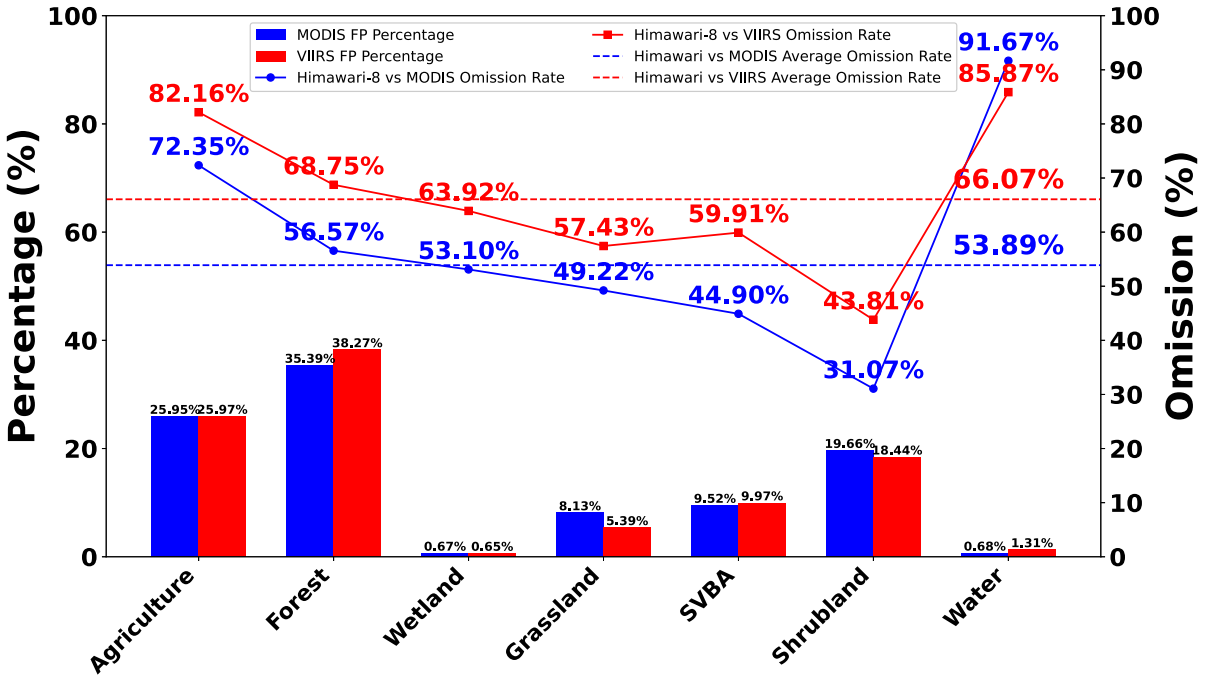

Fig. 7. The omission rate and fire point percentage of Himawari-8 wildfire products, under different land cover types according to the spatio-temporal matching of MODIS and VIIRS wildfire products. The blue bars represent the proportion of MODIS number of fire hotspots in different land cover types. The red bars represent the proportion of VIIRS number of fire hotspots in different land cover types.

spatial resolution of VIIRS wildfire products is highest with 375 m. This advantage allows VIIRS to detect small fires. In general, it is difficult to detect these small fires by MODIS and Himawari-8 (Jang et al., 2019). Comparing with VIIRS wildfire products, Himawari-8 wildfire products miss fewer fire hotspots using MODIS wildfire products as the reference data.

The omission rate of Himawari-8 wildfire products in Fig. 6 gradually increases at the beginning of the year, reaching the peak in February. The omission rate of Himawari-8 compared with MODIS wildfire products reaches 68.87%, while the omission rate compared with VIIRS wildfire products reaches 81.30%. In June, the omission rate rises in small increments, and then comes down. In November, the omission rate is the lowest in the whole year, and then shows an upward trend in December.

The main reason is that climate in most regions of the northern hemisphere is usually cold in February. Wildfires at this stage are dominated by low-intensity and low-temperature fires, which cause a wide range of missing detection for Himawari-8 wildfire products (Chuvieco et al., 2020). The southern hemisphere is summer in February when vegetation is lusher (Benger and Chapman, 2023). The observation angle of Himawari-8 is easily affected by the position of the sun (Ma et al., 2020), which results in a decrease for the detection accuracy of fire hotspots. In November, the southern hemisphere is in late spring and early summer when the weather is usually clear. It reduces cloud interference for satellite wildfire detection. In both the northern and southern hemispheres, surface temperatures are moderate. There is usually a large difference between the fire hotspot pixel and its neighborhood pixel. Therefore, the context algorithm could more effectively distinguish the fire hotspot pixel from the non-fire hotspot pixel, so as to reduce the omission rate of the wildfire detection.

(b) Verifying and analyzing Himawari-8 wildfire products under different land cover types

Fig. 7 depicts the omission rate and fire hotspot percentage of Himawari-8 wildfire products, compared with MODIS and VIIRS wildfire products under different land cover types. From the perspective of the number of fire hotspots, whether MODIS or VIIRS wildfire products, the proportion of fire hotspots in forest regions is the highest among all the land cover types, with 35.39% for MODIS and 38.27% for VIIRS. The proportion of fire hotspots in agriculture regions ranks second, with 25.95% for MODIS and 25.97% for VIIRS. Fire points in shrubland regions also account for a large part, with 19.66% and 18.44% in MODIS and VIIRS, respectively.

In general, forests have more vegetation areas, which are usually more flammable in the dry season (Dawson et al., 2001; Li et al., 2021). Therefore, high temperature and dryness tend to increase the fire risk of forests. In addition, lightning fire, man-made fire, and fire caused by power line short-circuit are also widespread in the forest regions (Veraverbeke et al., 2017).

Agricultural fires are common in East Asia, Southeast Asia, Australia and other regions (Li et al., 2014). In some specific periods, farmers may burn crops to prepare for the new season of crops. In addition, agricultural machines are also prone to sparks under high temperature and dry conditions, which may also cause wildfires (Val-Aguasca et al., 2019).

Shrubland is mainly composed of trees and shrubs, which usually contains more oil in these plants and vegetation (Valencia

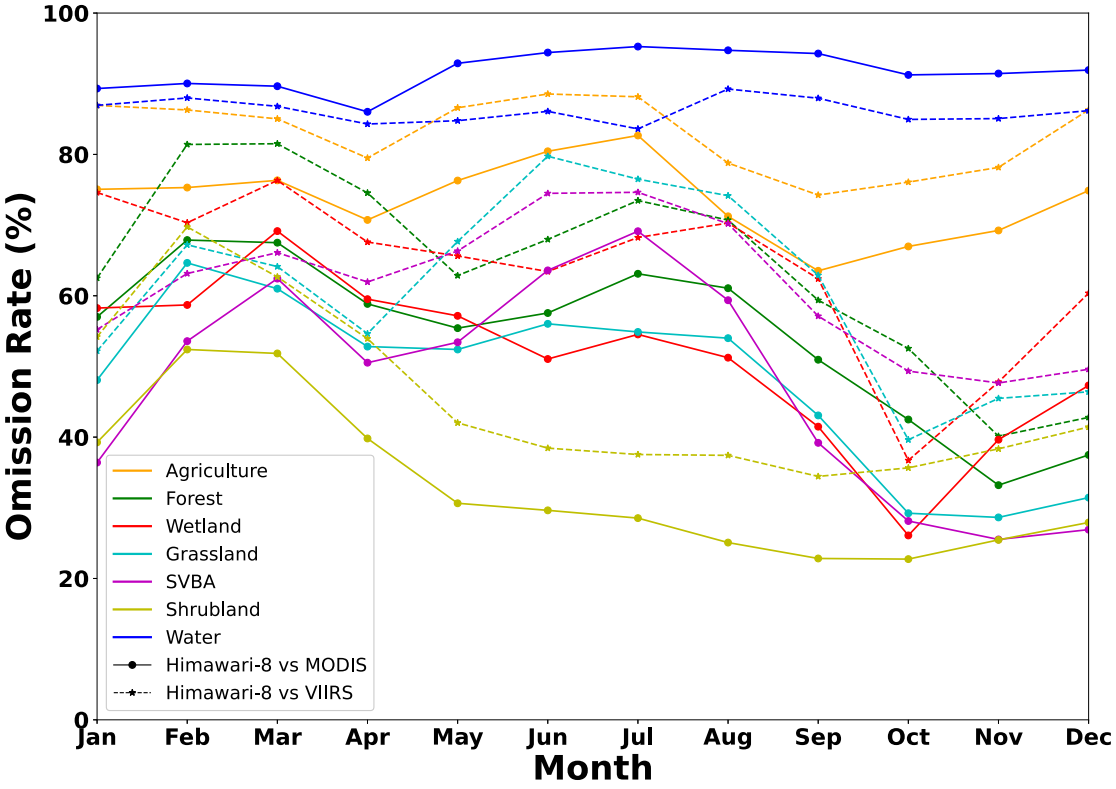

Fig. 8. The omission rate of Himawari-8 wildfire products, under both different months and different land cover types according to the spatio-temporal matching of MODIS and VIIRS wildfire products.

et al., 2023). The large number of fallen leaves on the ground is also a natural fuel, which is conducive to the occurrence and rapid spread of wildfires (Fonda, 2001).

Wetland, grassland, sparse vegetation and bare areas (SVBA in Fig. 7) account for a relatively small percentage of fire hotspots, with fire hotspots of MODIS and VIIRS wildfire products for 19% and 17.32%, respectively. Grassland is covered with herbaceous plants, which generally have a higher water content than woody plants. Therefore, herbs usually have a higher ignition point and are not easy to burn in a short period of time (Dimitrakopoulos and Bemmerzouk, 2003). Compared with bush and forest, grassland has a relatively low density of vegetation (Robles et al., 2024), where the fire is not easy to spread quickly (Archibald et al., 2018). A significant feature of wetland ecosystem is that plants in this area contain a lot of water and have a high ignition point (Guo et al., 2017). Even in dry climate, it is difficult to burn a large area in wetland, which greatly reduces the probability and spread of wildfires. In SVBA, the sparse vegetation is difficult to provide the combustible conditions that generate fire occurrence. The number of fire hotspots is naturally low. Water fires include fires on coastal facilities and ships. The high humidity environment and water coverage naturally inhibit the occurrence and spread of wildfires (Archibald et al., 2009).

In this study, water fires is an abbreviation for fire in and around water areas (Giglio et al., 2016). In Fig. 7, Himawari-8 has the highest omission rate in water fires, which is the only land cover type in comparison to MODIS and VIIRS, with 91.67% and 85.87%, respectively. The fire size in the water area is generally small, which is usually not conducive to Himawari-8. Among the land cover types with high fire incidence, Himawari-8 has a high fire hotspot omission rate in the agriculture areas. The omission rates compared with MODIS and VIIRS fire products are higher than the average value for all land cover types. The main reason is that agricultural fires are usually small (Korontzi et al., 2006). These agricultural fires are typically less than the individual pixel size of Himawari-8, resulting in massive missing of fire hotspots (Chen et al., 2022).

In forest area, the omission rate Himawari-8 is slightly higher than the average omission rate. Because of the dense vegetation in the forest, the fire hotspot may be obscured by the tree canopy (Siegert and Hoffmann, 2000), which is particularly unfavorable for Himawari-8 with low spatial resolution. In addition, the large amount of smoke produced by forest fires may also block the flame (Alarie, 2002; Zhang et al., 2020), which cause the missing detection of fire hotspots.

Compared with agriculture and forest, Himawari-8 has a lower omission rate in the shrubland regions. The reason is that shrubland is shorter and less dense than the forest (Whittaker, 1970), which is more obvious in the event of wildfires. Therefore, it is easier for Himawari-8 to detect the fire hotspot.

As portrayed in Fig. 8, this work presents the omission rate of Himawari-8 fire products, under both different months and different land cover types. In addition to the water regions, the change of fire hotspot omission rate is similar to that of the other land cover

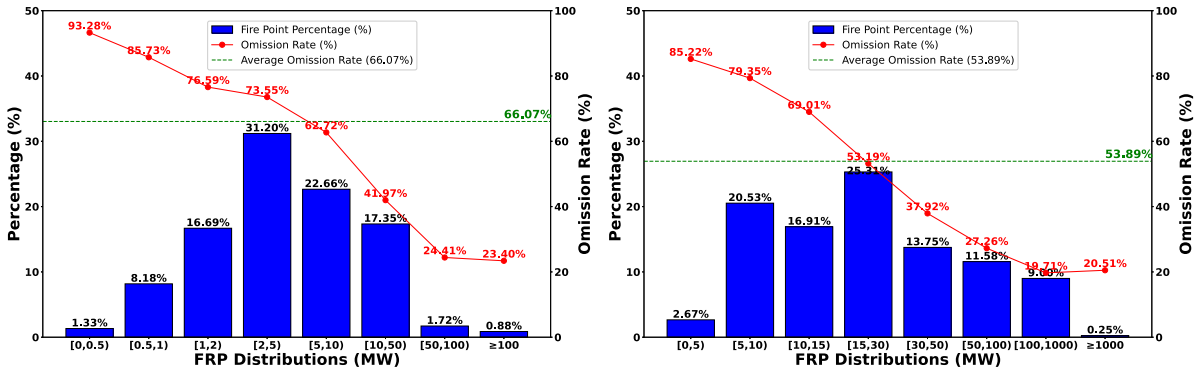

(a) Compared Himawari-8 with VIIRS wildfire products. **(b)** Compared Himawari-8 with MODIS wildfire products.

Fig. 9. The omission rate and fire hotspot percentage of Himawari-8 wildfire products, under different FRP distributions according to the spatio-temporal matching of MODIS and VIIRS wildfire products.

types in different months, especially at the beginning of the year when the omission rate is higher. The main reason is that fire hotspots in the water regions are generally not subject to seasonal variation (Pettit and Naiman, 2007), which does not affect the omission rate of Himawari-8 wildfire products.

(c) Verifying and analyzing Himawari-8 wildfire products under different FRP distributions

FRP directly represents the intensity and scale of the wildfire (Chatzopoulos-Vouzoglanis et al., 2024). In general, the higher the FRP estimates, the stronger the wildfire is. Compared with MODIS and VIIRS wildfire products under different FRP distributions, Fig. 9 reveals the omission rate of Himawari-8 wildfire products. With the increasing of FRP, the missing rate of Himawari-8 wildfire products is lower and lower. Compared with VIIRS, when the FRP range of fire hotspot is [0,0.5) MW, the omission rate is the highest with 93.28%. When FRP exceeds 100 MW, the omission rate is lower to 23.40%. Compared with MODIS, the omission rate ranges from the highest value 85.22% to the lowest value 19.72%. However, the lowest omission rate occurs in the regions where the FRP distribution is [100,1000] MW, rather than the regions where the FRP distribution is the highest. High FRP point is easy to be detected by Himawari-8. Moreover, the larger the fire size is, the higher the FRP estimates. Compared Himawari-8 with MODIS wildfire products, the omission rate gradually increases in the FRP exceeding 1000 range. The main reason is that when high-intensity wildfire occurs, it tends to generate a lot of accompanying smoke. The smoke may hinder the observation of satellite sensors. This causes the interference to wildfire detection algorithm, which leads to the missing detection of fire hotspot.

3.2.4. Comparisons on the frequency distributions of FRP

Considering that FRP is an indicator of fire intensity, section3.2.4–3.2.6 specifically compares FRP of Himawari-8 wildfire products with MODIS/VIIRS during 2022. The purpose is to further analyze the ability of these three wildfire products on retrieving FRP. Firstly, the frequency distributions of FRP in Himawari-8 and MODIS/VIIRS wildfire products are compared in Section 3.2.4. Secondly, comparisons on the spatio-temporal matching FRP are carried out in Section 3.2.5. Finally, comparisons on the frequency distributions of FRP under different land cover types are also analyzed in Section 3.2.6.

Fig. 10 shows the comparisons on the frequency distributions of FRP between Himawari-8 and MODIS/VIIRS wildfire products during 2022. Compared with VIIRS wildfire products in Fig. 10(a), the frequency distribution of FRP for Himawari-8 wildfire products is quite different in Fig. 10(c). The FRP distribution of Himawari-8 wildfire products ranges from 5 MW to 10 MW, while the FRP distribution of VIIRS wildfire products ranges from 1 MW to 2 MW. In addition, the FRP values of most Himawari-8 wildfire products (82.60%) are within 50 MW. While the FRP values of most VIIRS wildfire products (82.80%) are within 10 MW. The main reason for this difference in FRP distribution is the difference in satellite sensors. The Himawari-8 sensor has a lower spatial resolution of 2 km. VIIRS has a higher spatial resolution of 375 m. Statistically speaking, smaller pixels have a lower proportion of mixed pixels, which could better identify the fire hotspots of low FRP (Morisette et al., 2005). Therefore, VIIRS has the best wildfire detection performance for small fires. On the contrary, for small agricultural fires, Himawari-8 not performs dominant for this scene.

As demonstrated in Fig. 10, there is a high consistency of FRP between Himawari-8 and MODIS wildfire products, where most of the fire hotspots are distributed in 5 to 10 MW range. However, MODIS has a higher FRP frequency in this range than Himawari-8. The FRP values of most fire hotspots (83.78%) of MODIS wildfire products are also distributed in the range of 50 MW. It is worth noting that MODIS is more sensitive to the fire hotspots of FRP in 1 0MW range than Himawari-8. For FRP in the range of 0 to 5 MW, Himawari-8 has a higher proportion than MODIS. It is mainly due to the higher frequency of observation for Himawari-8. Himawari-8 owns more opportunities to observe small fires which end quickly (Xu and Zhong, 2017).

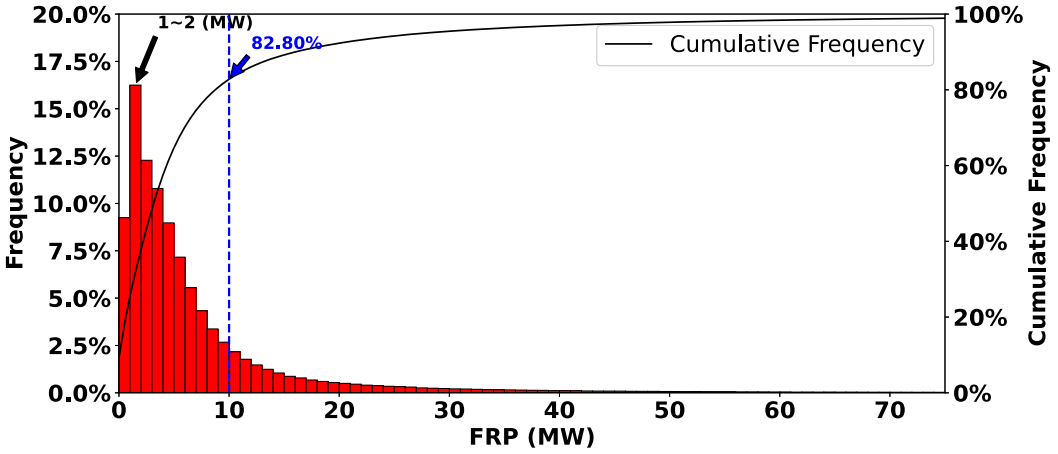

(**a**) Frequency distribution of FRP for VIIRS wildfire products.

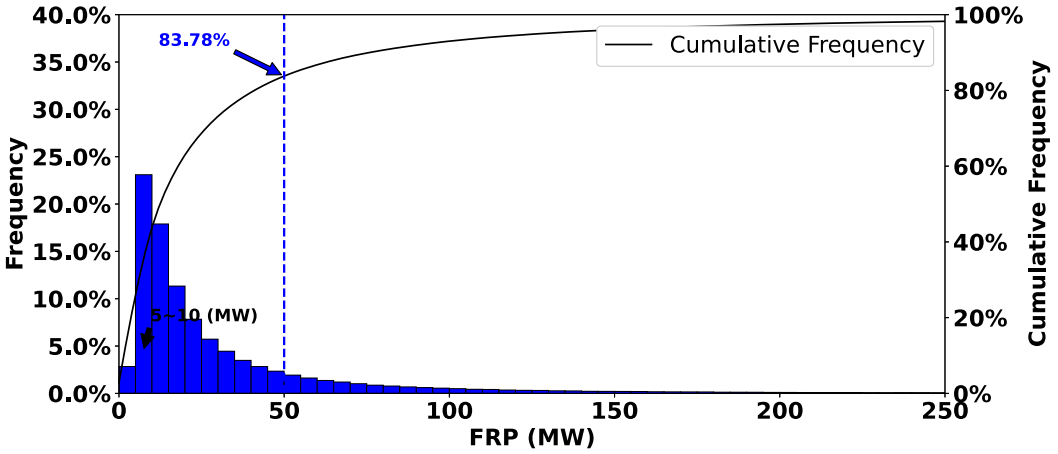

(**b**) Frequency distribution of FRP for MODIS wildfire products.

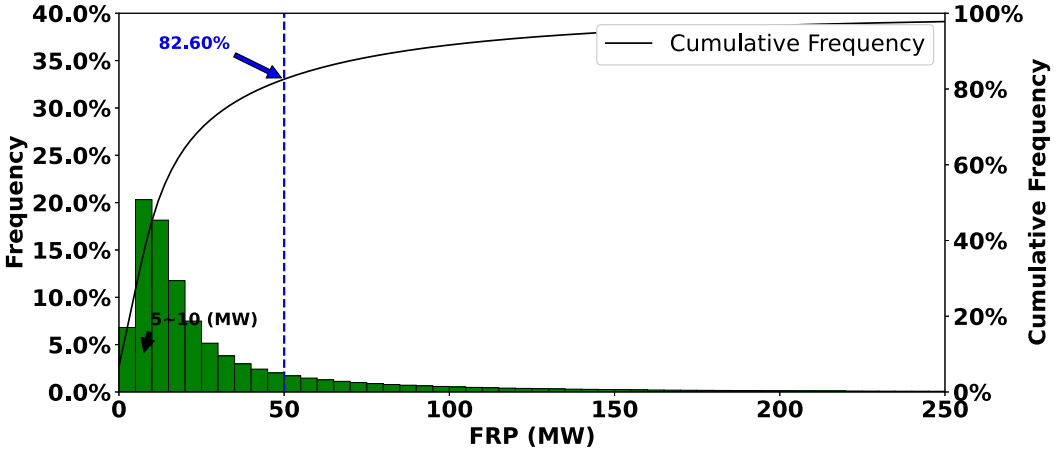

(**c**) Frequency distribution of FRP for Himawari-8 wildfire products.

Fig. 10. Comparisons on the frequency distributions of FRP between Himawari-8 and MODIS/VIIRS wildfire products during 2022.

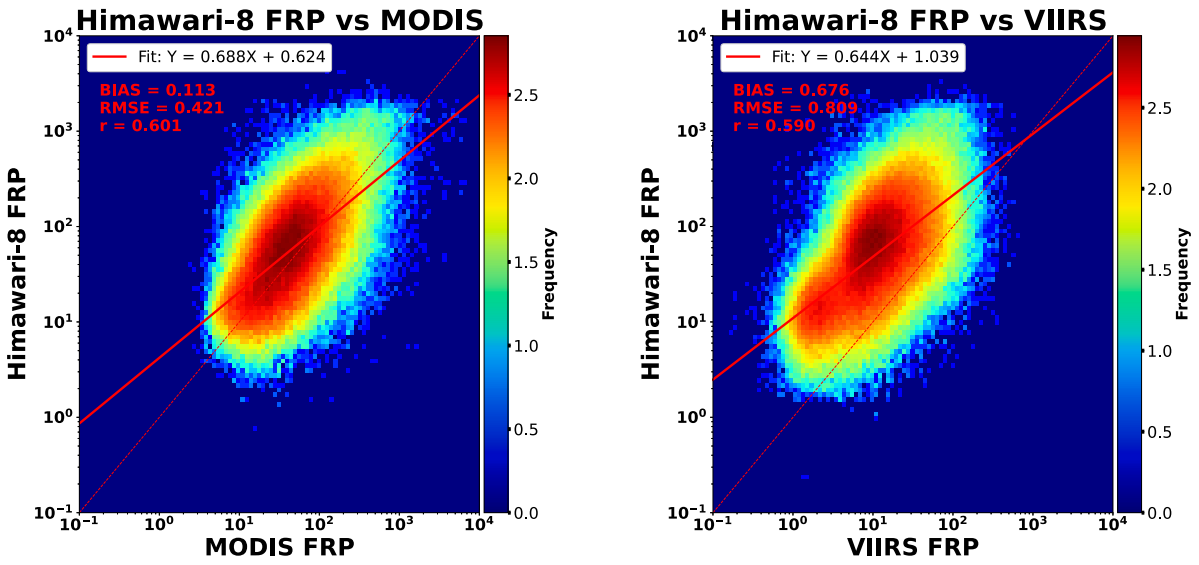

(a) MODIS FRP. (b) VIIRS FRP.

Fig. 11. The scatter plots of comparisons on the spatio-temporal matching FRP for Himawari-8 and MODIS/VIIRS wildfire products.

3.2.5. Comparisons on the FRP of spatio-temporal matching fire points

Fig. 11 reveals the scatter plots of comparisons on the spatio-temporal matching FRP for Himawari-8 and MODIS/VIIRS wildfire products. Obviously, compared with MODIS and VIIRS wildfire products, the FRP estimation of Himawari-8 is generally higher. The comparisons with VIIRS are usually over-estimated than the comparisons with MODIS. The RMSE of FRP estimations for Himawari-8 wildfire products are 0.421 and 0.809, compared with MODIS and VIIRS, respectively. It indicates a stronger FRP correlation between Himawari-8 and MODIS wildfire products. This is mainly due to the spatial resolution of Himawari-8 is 2 km, while MODIS is 1 km, and VIIRS is 375 m. Therefore, VIIRS could more finely estimate the FRP values of the fire hotspot than MODIS and Himawari-8. The larger pixel areas include more mixing pixels with different types (Foody and Cox, 1994), which leads to the over-estimation of FRP value.

3.2.6. Comparisons on the FRP of spatio-temporal matching fire points under different land cover types

Fig. 12 shows the scatter plots of comparisons on the spatio-temporal matching FRP for Himawari-8 and MODIS/VIIRS wildfire products under different land cover types (Forest, Agriculture and Shrubland). The largest RMSE of FRP for the three wildfire products is shrubland regions, while the smallest RMSE of FRP is the agriculture regions. In other words, the estimating of FRP for Himawari-8 wildfire products under shrubland regions is high. The main reason is that the shrubland regions are mostly shrubs and low trees, and its fire characteristics are high temperature and long duration (Moritz, 2003). Whereas the pixel area of Himawari-8 is the largest, which usually leads to over-estimation of FRP in shrubland regions.

In contrast, the estimated FRP values of Himawari-8 wildfire products perform the best in agriculture regions. This is mainly because most of the fire hotspots in agriculture regions are agricultural artificial activities such as straw burning. The characteristics of the wildfire behave low temperature and short duration (Vadrevu et al., 2011). The ability of Himawari-8 to detect small agriculture fire hotspots is generally weak. Nevertheless, it shows the most stable performance in FRP estimation for agriculture regions. The main reason is that the burning regions of most agriculture fires are much smaller than the single pixel size of Himawari-8. Moreover, the combustion temperature is relatively low, which reduces the proportion of high temperature pixels in Himawari-8. Thus it inhibits the over-estimation of FRP for Himawari-8 wildfire products.

3.3. Compared Himawari-8 with Himawari-9 wildfire products

Himawari-9 is the successor satellite of Himawari-8, which completely replaced Himawari-8 after December 2022. It is worth noting that during the transition period from October to November 2022, both Himawari-8 and Himawari-9 satellites are carried out the wildfire detection missions at the same time. Therefore, in this period, we could compare and analyze the two same sensors Himawari-8 and Himawari-9 for the wildfire products. Firstly, the fire hotspots of the two wildfire products are executed spatio-temporal matching operation. The principle of spatio-temporal matching is that the haversine distance is limited within 2.5 km, and there is at least one fire hotspot within 10 min before and after the moment. In addition, this work also processes them with MODIS/VIIRS wildfire products via spatio-temporal matching. The wildfire detection capability and differences of the new Himawari-9 satellite and the old Himawari-8 satellite are analyzed as follows.

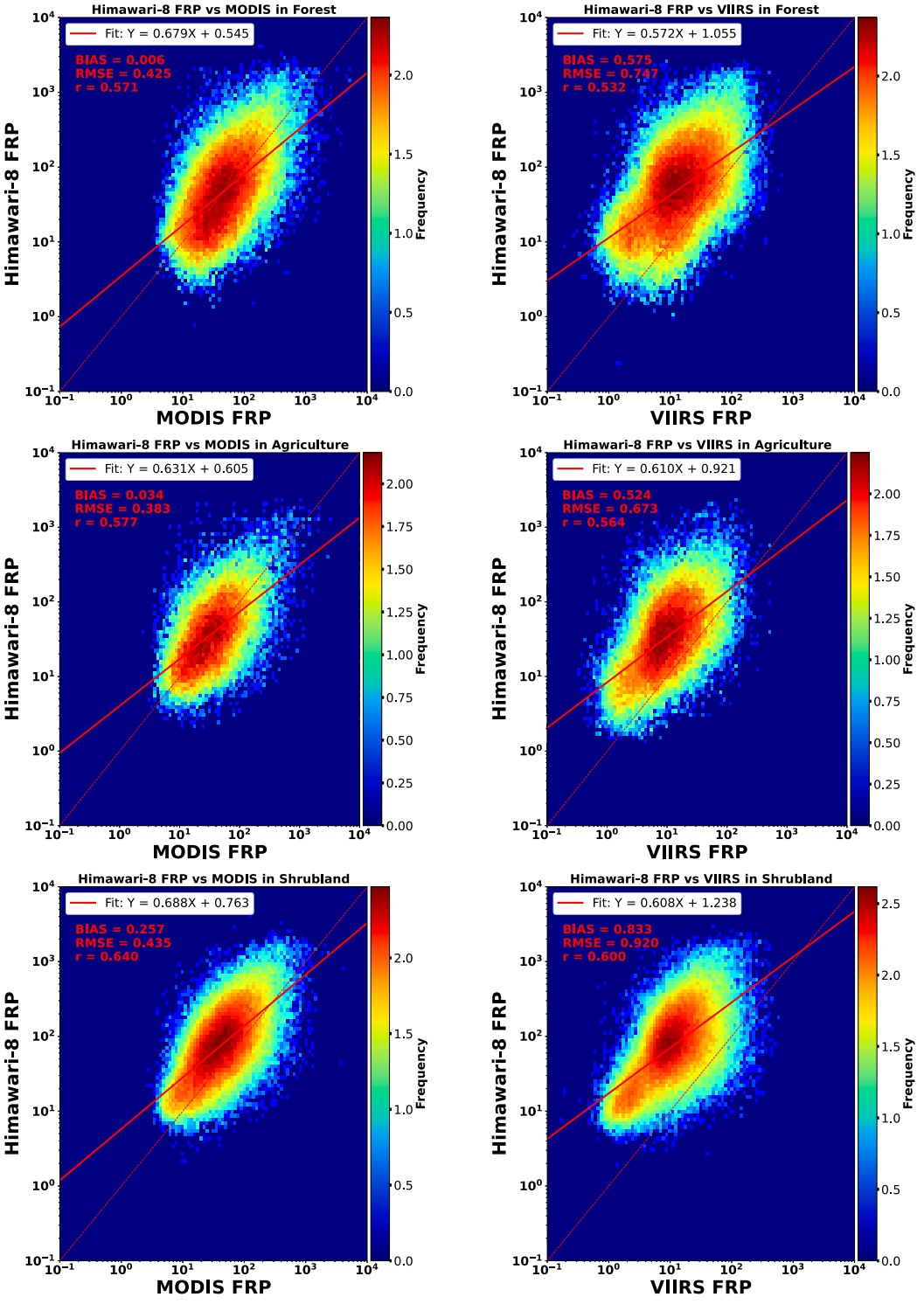

Fig. 12. The scatter plots of comparisons on the spatio-temporal matching FRP for Himawari-8 and MODIS/VIIRS wildfire products under different land cover types (Forest, Agriculture and Shrubland).

Table 2
The omission rate of Himawari-8 versus Himawari-9 with MODIS/VIIRS wildfire products during October and November 2022.

Products	2022.10-MODIS	2022.10-VIIRS	2022.11-MODIS	2022.11-VIIRS	2023.10-MODIS	2023.11-MODIS
Himawari-8	**39.21**	**55.49**	**39.61**	**56.19**	–	–
Himawari-9	42.53	56.99	41.46	56.62	**34.81**	**35.78**

Table 3
The consistency of Himawari-8 versus Himawari-9 during October and November 2022.

Products	2022.10	2022.11
Himawari-8	66.50	73.13
Himawari-9	**71.46**	**78.48**

As listed in Table 2, the omission rate of Himawari-8 versus Himawari-9 with MODIS/VIIRS wildfire products is given during October to November 2022. In terms of the omission rate, there are slight differences between Himawari-8 and Himawari-9. The omission rate of Himawari-9 is higher than that of Himawari-8. In October and November 2023, Himawari-8 has no observed data. Nevertheless, the omission rate of Himawari-9 compared with MODIS in 2023, is lower than that of Himawari-8 compared with MODIS in the same month in 2022. In Table 3, from the perspective of the Himawari-9 wildfire products, the consistency with Himawari-8 wildfire products is strong. However, from the perspective of Himawari-8 wildfire products, the consistency with Himawari-9 wildfire products is weak. Overall, Himawari-9 could detect more fire hotspots than Himawari-8. Himawari-8 detected 1 986 983 and 1 723 015 fire hotspots in October and November 2022, respectively. During the same period, Himawari-9 detected 2 236 645 and 1 926 072 fire hotspots, respectively.

According to the above results, Himawari-9 could detect more fire hotspots than Himawari-8. The main reason is due to Himawari-9 owns newer sensor in contrast with Himawari-8 (Bessho et al., 2016). However, Himawari-9 has a higher omission rate than Himawari-8, indicating that there are more false fire hotspots detected by Himawari-9. Because Himawari-9 is still in debugging and calibration phase in 2022, resulting in its initial slightly lower performance than Himawari-8. In November 2022, the omission rate of Himawari-8 compared with MODIS/VIIRS is higher than the omission rate in October 2022. Nevertheless, the omission rate of Himawari-9 compared with MODIS/VIIRS is lower than the omission rate in October 2022. Over time, the performance of Himawari-9 has continuously improved after continuous debugging and calibration.

From the perspective of Himawari-8/9 compared with MODIS/VIIRS wildfire products, the average omission rate of Himawari-9 compared with MODIS in October and November 2022 is 41.97%, and the average omission rate of Himawari-9 compared with VIIRS in the same period is 56.81%. The average omission rate of Himawari-8 compared with MODIS in October and November 2022 is 39.42%, and the average omission rate of Himawari-8 compared with VIIRS in the same period is 55.84%. Himawari-9 compares MODIS with an average omission rate of 2.55%, which is higher than Himawari-8. The average omission rate of Himawari-9 compared with VIIRS is only 0.97% higher than that of Himawari-8. This is due to VIIRS has a higher spatial resolution than MODIS, which theoretically has better wildfire detection accuracy (Fang et al., 2021). Himawari-9 shows slight difference from Himawari-8 in its early operation. It indicates that the high omission rate of Himawari-9 may be due to the errors of MODIS/VIIRS wildfire detection (Fu et al., 2020).

3.4. Validation of Himawari-8/9 wildfire products based on ground truth fire data

This study uses ground truth fire data to validate the real fire detection potential of the Himawari satellites. Himawari-8/9 observes the full disk every 10 min, aiming to monitor fires in near real-time. Firstly, this module discusses the missed detection of ground truth fires by the Himawari-8/9 wildfire products. This module first analyzes the omission of ground truth fires by the Himawari-8/9 wildfire products. Secondly, the fire detection capability of geostationary satellites depends not only on whether fires could be detected, but also on the delay in detecting fires. It is generally believed that successful detection within 10 min of the report time or detection before the report is considered to indicate strong near real-time detection capability. Successful detection of fires within 60 min of the report time is considered to indicate moderate near real-time detection capability. Successful detection of fires after 60 min of the report time is considered to indicate poor near-real-time detection capability. Successful detection of fires within 60 min is considered as near real-time detection.

Fig. 13 depicts the performance of Himawari-8/9 wildfire products on detecting ground truth fires. It shows the number of fires undetected by Himawari-8/9 wildfire products, as well as the number of fires detected before the report time, within 10 min, within 60 min and after 60 min.

Firstly, the omission of ground truth fires by Himawari-8/9 wildfire products is analyzed. Out of 70 fire report incidents, the Himawari-8/9 wildfire products miss only 14 fires, resulting in an omission rate of just 20%. The 14 fire incidents missed by the Himawari-8/9 wildfire products have an average damaged area of 4.61 ha, with 10 of these incidents having a damaged area of less than 1 ha. The largest damaged area is only 18.5 ha. Obviously, the damaged area of all ground truth fire incidents missed by the Himawari-8/9 wildfire products is much smaller than the size of a single AHI pixel. Even the largest damaged area among the

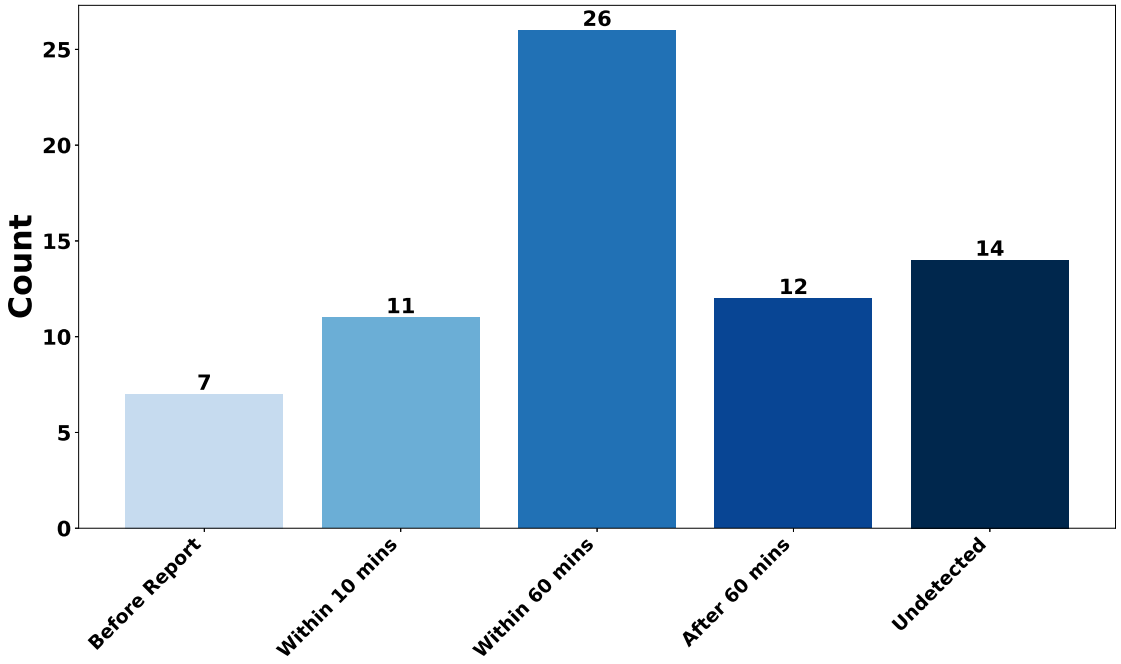

Fig. 13. The performance of Himawari-8/9 wildfire products on detecting ground truth fires.

missed fires only accounts for 4.63% of a single AHI pixel. The small damaged area of fires causing satellite detection omissions is a weakness common to all satellite-based fire detection systems. However, due to the coarse spatial resolution of AHI, this disadvantage is further amplified.

Secondly, the detection delay of the 56 ground truth fire incidents successfully detected by the Himawari-8/9 wildfire products is analyzed. Among them, most of the fires fall within the "Within 60 minutes" interval. Only 12 fires fall into the "After 60 minutes" interval, accounting for 21.43% of the successfully detected fires. Generally, successful detection of fires within 60 min is considered as near real-time detection. Among these 56 fire incidents, 44 incidents meet the near real-time detection standard, accounting for 78.57% of the successfully detected fires. It indicates that Himawari-8/9 has a strong near real-time wildfire detection capability and is fully capable of performing near real-time wildfire detection tasks.

4. Conclusions and prospects

4.1. Conclusions

In order to verify the effectiveness of Himawari-8/9 wildfire products, this work uses the wildfire products of MODIS and VIIRS, two high spatial resolution polar-orbiting satellites, and related auxiliary data for comparison and validation. The main conclusions are summarized as follows:

(1) Analyzing the fire hotspots of Himawari-8, MODIS and VIIRS wildfire products in April 2015 to December 2022. The three satellite wildfire products show strong similarity. Among them, Himawari-8 wildfire products detect the most fire hotspots due to its high temporal resolution. Moreover, VIIRS wildfire products detect the more fire hotspots than MODIS, because of its high spatial resolution.

(2) Analyzing the spatial distribution of fire hotspots for three satellite wildfire products in Sichuan Province, China, from 2020 to 2022. Himawari-8, MODIS and VIIRS wildfire products all have a large number of fire hotspots clustered in the southern of Sichuan. In Chengdu city, both MODIS and VIIRS wildfire products cluster different degrees of fire hotspots, while Himawari-8 does not exist this phenomenon. The spatial distribution of MODIS and VIIRS wildfire products is more similar. However, there is no strong similarity between Himawari-8 and MODIS/VIIRS wildfire products in terms of the spatial distribution. The main reason is that MODIS and VIIRS have strong similarities in sensor and algorithm design (Coskuner, 2022), whereas Himawari-8 is quite different from them.

(3) Comparing Himawari-8 with MODIS and VIIRS wildfire products under different months, different land cover types, and different FRP distributions from April 2015 to December 2022.

Under different months: the omission rate of Himawari-8 comparison on MODIS and comparison on VIIRS wildfire products are relatively similar under different months. Himawari-8 shows a higher omission rate in February and March. Compared with MODIS, it is 68.87% and 63.68% in February and March, respectively. Compared with VIIRS, it is 81.30% and 79.69% in February

and March, respectively. In November, the lowest omission rate of the whole year is 36.11% comparison on MODIS and 49.63% comparison on VIIRS. The main reason for this difference in omission rate between different months is climate change, environmental change and human activity (Jolly et al., 2015; Westerling et al., 2006), and the angle of the sun.

Under different land cover types: forest fires, agriculture fires and shrubland fires account for a large proportion of all fires. Himawari-8 shows the weakest detection ability for water fires, with omission rates of 91.67% and 85.87% compared with MODIS and VIIRS, respectively. Himawari-8 has the best wildfire detection performance in shrubland area, where the omission rate is 31.07% and 43.81% compared with MODIS and VIIRS, respectively. In other land cover types, the wildfire detection performance of agriculture and forest regions is lower than the average level. In addition, except for water regions, the frequency of fires varies on the seasons, which affects the wildfire detection performance of Himawari-8.

Under different FRP distributions: Himawari-8 behaves strong similarity to MODIS and VIIRS wildfire products. With the increasing of FRP, the omission rate of Himawari-8 wildfire products is lower and lower. It indicates that Himawari-8 has the better detection ability for high -intensity fires. However, for ultra-high intensity fires, Himawari-8 may be obscured by the smoke of the fire, resulting in more missing fire hotspots.

(4) Comparing FRP of Himawari-8 wildfire products with MODIS/VIIRS during 2022. Firstly, for the FRP distribution, Himawari-8 and MODIS show a strong similarity. However, VIIRS has a different situation whose FRP are mainly concentrated within 10 MW, and it has the most FRP distribution in 1 to 2 MW. Then, the fire hotspots of Himawari-8 which are spatio-temporal matched with MODIS and VIIRS wildfire products are analyzed. It is found that FRP values retrieval for Himawari-8 has the better consistency than VIIRS. The RMSE of FRP values retrieval for Himawari-8 compared with MODIS and VIIRS is 0.421 and 0.809, respectively. However, Himawari-8 over-estimates FRP values compared with both MODIS and VIIRS. Himawari-8 has the best FRP values estimating in agriculture regions and the worst in shrubland regions.

(5) Analyzing the performance on wildfire detection of old Himawari-8 and new Himawari-9 satellite in the same period. In terms of Himawari-9, its consistency with Himawari-8 is slightly stronger. From the perspective of Himawari-8, its consistency with Himawari-9 is slightly weaker. However, from the perspective of MODIS and VIIRS, Himawari-8 has a lower omission rate. This is mainly due to that Himawari-9 is still in the early stage of debugging and calibration. With the continuous debugging and calibration, the omission rate of Himawari-9 wildfire products begins to decrease, indicating that the wildfire detection performance of Himawari-9 is gradually improving.

(6) This paper analyzes the omission of ground truth fire data by Himawari-8/9 wildfire products and their near real-time wildfire detection capability. Overall, the Himawari-8/9 wildfire products perform well in detecting these 70 fire incidents. However, some fires with small damaged areas are missed, which is an inherent limitation of satellite-based fire detection. From the analysis of detection delays, 78.57% of the fire incidents are detected within 60 min after the report time. It indicates that Himawari-8/9 is fully capable of performing near real-time wildfire detection tasks.

This work discuss the similarities and differences between the old and new versions of MODIS and VIIRS fire products in this section. According to the clear instructions in the guides (Giglio et al., 2021; Schroeder et al., 2025), there are no changes in core algorithms or product structures between the fire hotspots products of MODIS C6 and MODIS C6.1. Only minor differences are caused by the calibration updates of the red band (Band 1) and near-infrared band (Band 2) of the upstream Level-1B radiance products. The original statement in the guide is given as follows: "The MODIS active fire products are among those for which no algorithm or product changes were made for Collection 6.1, and as such the Collection-6 and Collection-6.1 active fire products are sufficiently consistent to the extent that they may be freely intermixed". The main improvements of VIIRS C2 focus on upstream data quality optimization. It adds new quality flags and optimizes file compression. The core fire hotspots detection logic has not been fundamentally adjusted. Key parameters and thresholds remain consistent.

To confirm that the core fire hotspots detection logic of the MODIS C6.1 and VIIRS C2 fire products has not been fundamentally adjusted, and to prove that the MODIS C6 and VIIRS C1 data are scientifically and accurately equivalent to the new versions, we conducted the following experiment. We selected the 2021 fire hotspots product data of MODIS C6.1, VIIRS C2 and Himawari-8. We followed the original spatio-temporal matching rules of the paper. We recalculated the monthly omission rate of the Himawari-8 fire products. The experimental results are shown in Table 4. From the experimental results, we found that the omission rate derived from MODIS C6 and MODIS C6.1 is completely consistent. The omission rate derived from VIIRS C2 and VIIRS C1 differs by less than 0.5%. Therefore, the MODIS C6 and VIIRS C1 data are completely equivalent to the new versions in terms of scientificity and accuracy. There is no situation where “new versions are better” and thus old versions become unusable.

4.2. Prospects

In summary, this work validates and compares Himawari-8/9 10-minute wildfire products with MODIS/VIIRS wildfire products. The validation work in this paper could provide the beneficial guides for the future wildfire detection and FRP retrieval algorithms as follows.

Firstly, for the future algorithms of Himawari-8/9 wildfire detection, the contextual methods are limited for early and small fires. Moreover, current Himawari-8/9 wildfire products ignore the temporal information, which is the strongest advantage of Himawari-8/9. Therefore, temporal, spatial and spectral information could be combined to fully exploit the feature of wildfire.

Secondly, according to the FRP retrieval of Himawari-8/9, the future wildfire detection algorithms need to focus on small fires and reduce the omission rate. For algorithm designing, it could replace the traditional context methods as machine learning and deep learning technology. Besides, VIIRS/MODIS wildfire products data could be regarded as the training data.

Table 4
The omission rate comparisons for VIIRS C1 vs C2, MODIS C6 vs MODIS C6.1 with Himawari-8.

Month	VIIRS C1	VIIRS C2	MODIS C6	MODIS C6.1
01	82.19%	82.25%	69.96%	69.96%
02	86.34%	86.42%	72.92%	72.92%
03	81.68%	81.80%	63.44%	63.44%
04	71.63%	71.84%	59.61%	59.61%
05	60.57%	60.75%	52.04%	52.04%
06	68.23%	68.18%	58.07%	58.07%
07	63.17%	63.40%	54.89%	54.89%
08	62.81%	62.79%	52.25%	52.25%
09	62.70%	62.89%	52.89%	52.89%
10	49.54%	49.62%	35.14%	35.14%
11	55.54%	55.77%	39.67%	39.67%
12	62.06%	62.41%	46.00%	46.00%

Thirdly, FRP retrieval algorithms should also take the different land cover types into account, especially for distinguishing the combustible and non-combustible regions. Based on this strategy, FRP retrieval algorithms could dynamically adjust parameters via different land cover types, to improve the retrieval accuracy.

Finally, Himawari-8/9 wildfire products would produce more serious omission in the thick smoke scenario. Therefore, detecting smoke could also be used as a way of detecting fires. Then this negative factor could be turned into positive factor to reduce the omission rate of Himawari-8/9 wildfire detection.

CRediT authorship contribution statement

Zifeng Liu: Writing – original draft, Validation, Resources, Data curation. **Qiang Zhang:** Writing – review & editing, Supervision, Methodology, Funding acquisition. **Baomo Zhang:** Writing – review & editing, Software, Resources, Formal analysis. **Jian Zhu:** Writing – review & editing, Software, Resources, Methodology.

Declaration of competing interest

The authors declare the following financial interests/personal relationships which may be considered as potential competing interests: Qiang Zhang reports financial support was provided by National Natural Science Foundation of China. If there are other authors, they declare that they have no known competing financial interests or personal relationships that could have appeared to influence the work reported in this paper.

Acknowledgments

This study is supported in part by the National Natural Science Foundation of China under Grant 62401095; And in part by the Dalian Science and Technology Talent Innovation Supporting Project under Grant 2024RQ028; And in part by the China Postdoctoral Science Foundation under Grant 2023M740460 and 2025T180065; And in part by the Natural Science Foundation of Liaoning Province under Grant 2025-BS-0236; And in part by the Fundamental Research Funds for the Central Universities under Grant 3132026267.

Data availability

Data will be made available on request.

References

Alarie, Y., 2002. Toxicity of fire smoke. Crit. Rev. Toxicol. 32 (4), 259–289.
Archibald, S., Lehmann, C.E., Belcher, C.M., Bond, W.J., Bradstock, R.A., Daniau, A.-L., Dexter, K.G., Forrestel, E.J., Greve, M., He, T., et al., 2018. Biological and geophysical feedbacks with fire in the earth system. Environ. Res. Lett. 13 (3), 033003.
Archibald, S., Roy, D.P., van Wilgen, B.W., Scholes, R.J., 2009. What limits fire? An examination of drivers of burnt area in Southern Africa. Global Change Biol. 15 (3), 613–630.
Aslan, Y.E., Korpeoglu, I., Ulusoy, Ö., 2012. A framework for use of wireless sensor networks in forest fire detection and monitoring. Comput. Environ. Urban Syst. 36 (6), 614–625.
Bastarrika, A., Chuvieco, E., Martín, M.P., 2011. Mapping burned areas from landsat TM/ETM+ data with a two-phase algorithm: Balancing omission and commission errors. Remote. Sens. Environ. 115 (4), 1003–1012.
Benger, N., Chapman, B., 2023. Seasonal climate summary for the southern hemisphere (summer 2019–20): a summer of extremes. J. South. Hemisph. Earth Syst. Sci. 73 (2), 83–101.
Bessho, K., Date, K., Hayashi, M., Ikeda, A., Imai, T., Inoue, H., Kumagai, Y., Miyakawa, T., Murata, H., Ohno, T., et al., 2016. An introduction to himawari-8/9—Japan's new-generation geostationary meteorological satellites. J. Meteorol. Soc. Jpn. Ser. II 94 (2), 151–183.

Bowman, D.M., Williamson, G.J., Abatzoglou, J.T., Kolden, C.A., Cochrane, M.A., Smith, A.M., 2017. Human exposure and sensitivity to globally extreme wildfire events. Nat. Ecol. Evol. 1 (3), 0058.
CCI, ESA Land Cover, 2017. Product user guide version 2.0. UCL-Geomatics: Lond. UK.
Chatzopoulos-Vouzoglanis, K., Reinke, K.J., Soto-Berelov, M., Jones, S.D., 2023. One year of near-continuous fire monitoring on a continental scale: Comparing fire radiative power from polar-orbiting and geostationary observations. Int. J. Appl. Earth Obs. Geoinf. 117, 103214.
Chatzopoulos-Vouzoglanis, K., Reinke, K.J., Soto-Berelov, M., Jones, S.D., 2024. Are fire intensity and burn severity associated? Advancing our understanding of FRP and NBR metrics from Himawari-8/9 and Sentinel-2. Int. J. Appl. Earth Obs. Geoinf. 127, 103673.
Chen, J., Li, R., Tao, M., Wang, L., Lin, C., Wang, J., Wang, L., Wang, Y., Chen, L., 2022. Overview of the performance of satellite fire products in China: Uncertainties and challenges. Atmospheric Environ. 268, 118838.
Chen, J., Lv, Q., Wu, S., Zeng, Y., Li, M., Chen, Z., Zhou, E., Zheng, W., Liu, C., Chen, X., et al., 2023. An adapted hourly himawari-8 fire product for China: principle, methodology and verification. Earth Syst. Sci. Data Discuss. 2023, 1–32.
Chuvieco, E., Aguado, I., Salas, J., García, M., Yebra, M., Oliva, P., 2020. Satellite remote sensing contributions to wildland fire science and management. Curr. For. Rep. 6, 81–96.
Coppo, P., 2015. Simulation of fire detection by infrared imagers from geostationary satellites. Remote Sens. Environ. 162, 84–98.
Coskuner, K.A., 2022. Assessing the performance of MODIS and VIIRS active fire products in the monitoring of wildfires: a case study in Turkey. IForest-Biogeosciences For. 15 (2), 85.
Cruz, H., Eckert, M., Meneses, J., Martínez, J.F., 2016. Efficient forest fire detection index for application in unmanned aerial systems (UASs). Sensors 16 (6), 893.
Cui, S., Song, Z., Zhang, L., Shen, Z., Hough, R., Zhang, Z., An, L., Fu, Q., Zhao, Y., Jia, Z., 2021. Spatial and temporal variations of open straw burning based on fire spots in northeast China from 2013 to 2017. Atmos. Environ. 244, 117962.
Dawson, T.P., Butt, N., Miller, F., 2001. The ecology of forest fires. ASEAN Biodivers.: Newsmag. ASEAN Reg. Cent. Biodivers. Conserv. 1 (3), 18–21.
Dimitrakopoulos, A., Bemmerzouk, A., 2003. Predicting live herbaceous moisture content from a seasonal drought index. Int. J. Biometeorol. 47, 73–79.
Fang, B., Lakshmi, V., Cosh, M.H., Hain, C., 2021. Very high spatial resolution downscaled SMAP radiometer soil moisture in the CONUS using VIIRS/MODIS data. IEEE J. Sel. Top. Appl. Earth Obs. Remote. Sens. 14, 4946–4965.
Fonda, R.W., 2001. Burning characteristics of needles from eight pine species. For. Sci. 47 (3), 390–396.
Foody, G., Cox, D., 1994. Sub-pixel land cover composition estimation using a linear mixture model and fuzzy membership functions. Remote. Sens. 15 (3), 619–631.
Fu, Y., Li, R., Wang, X., Bergeron, Y., Valeria, O., Chavardès, R.D., Wang, Y., Hu, J., 2020. Fire detection and fire radiative power in forests and low-biomass lands in northeast Asia: MODIS versus VIIRS fire products. Remote. Sens. 12 (18), 2870.
Giglio, L., Descloitres, J., Justice, C.O., Kaufman, Y.J., 2003. An enhanced contextual fire detection algorithm for MODIS. Remote. Sens. Environ. 87 (2–3), 273–282.
Giglio, L., Schroeder, W., Hall, J.V., Justice, C.O., 2021. MODIS Collection 6 and Collection 6.1 Active Fire Product User's Guide. National Aeronautical and Space Administration—NASA, Washington, DC, USA, p. 64.
Giglio, L., Schroeder, W., Justice, C.O., 2016. The collection 6 MODIS active fire detection algorithm and fire products. Remote. Sens. Environ. 178, 31–41.
Guo, M., Li, J., Sheng, C., Xu, J., Wu, L., 2017. A review of wetland remote sensing. Sensors 17 (4), 777.
Hantson, S., Padilla, M., Corti, D., Chuvieco, E., 2013. Strengths and weaknesses of MODIS hotspots to characterize global fire occurrence. Remote Sens. Environ. 131, 152–159.
Jang, E., Kang, Y., Im, J., Lee, D.W., Yoon, J., Kim, S.K., 2019. Detection and monitoring of forest fires using Himawari-8 geostationary satellite data in south Korea. Remote. Sens. 11 (3), 271.
Jolly, W.M., Cochrane, M.A., Freeborn, P.H., Holden, Z.A., Brown, T.J., Williamson, G.J., Bowman, D.M., 2015. Climate-induced variations in global wildfire danger from 1979 to 2013. Nat. Commun. 6 (1), 7537.
Justice, C., Giglio, L., Korontzi, S., Owens, J., Morisette, J., Roy, D., Descloitres, J., Alleaume, S., Petitcolin, F., Kaufman, Y., 2002. The MODIS fire products. Remote. Sens. Environ. 83 (1–2), 244–262.
Korontzi, S., McCarty, J., Loboda, T., Kumar, S., Justice, C., 2006. Global distribution of agricultural fires in croplands from 3 years of moderate resolution imaging spectroradiometer (MODIS) data. Glob. Biogeochem. Cycles 20 (2).
Li, P., Feng, Z., Jiang, L., Liao, C., Zhang, J., 2014. A review of swidden agriculture in southeast Asia. Remote. Sens. 6 (2), 1654–1683.
Li, L., Ma, Z., Cao, T., 2021. Data-driven investigations of using social media to aid evacuations amid western United States wildfire season. Fire Saf. J. 126, 103480.
Li, F., Zhang, X., Kondragunta, S., Schmidt, C.C., Holmes, C.D., 2020. A preliminary evaluation of GOES-16 active fire product using landsat-8 and VIIRS active fire data, and ground-based prescribed fire records. Remote Sens. Environ. 237, 111600.
Ma, X., Huete, A., Tran, N.N., Bi, J., Gao, S., Zeng, Y., 2020. Sun-angle effects on remote-sensing phenology observed and modelled using himawari-8. Remote. Sens. 12 (8), 1339.
Mitchell, J.W., 2023. Analysis of utility wildfire risk assessments and mitigations in California. Fire Saf. J. 140, 103879.
Mohapatra, A., Trinh, T., 2022. Early wildfire detection technologies in practice—a review. Sustainability 14 (19), 12270.
Morisette, J.T., Giglio, L., Csiszar, I., Setzer, A., Schroeder, W., Morton, D., Justice, C.O., 2005. Validation of MODIS active fire detection products derived from two algorithms. Earth Interactions 9 (9), 1–25.
Moritz, M.A., 2003. Spatiotemporal analysis of controls on shrubland fire regimes: age dependency and fire hazard. Ecology 84 (2), 351–361.
Moritz, M.A., Batllori, E., Bradstock, R.A., Gill, A.M., Handmer, J., Hessburg, P.F., Leonard, J., McCaffrey, S., Odion, D.C., Schoennagel, T., et al., 2014. Learning to coexist with wildfire. Nature 515 (7525), 58–66.
Pettit, N.E., Naiman, R.J., 2007. Fire in the riparian zone: characteristics and ecological consequences. Ecosystems 10, 673–687.
Robles, D., Bergeron, Y., Meunier, J., Stambaugh, M., Raymond, P., Kryshen, A., Goebel, C., Eden, J., Drobyshev, I., 2024. Climatic controls of fire activity in the red pine forests of eastern North America. Agricult. Forest. Meterol. 358, 110219.
Schroeder, W., Giglio, L., 2018. NASA VIIRS land science investigator processing system (SIPS) visible infrared imaging radiometer suite (VIIRS) 375 m & 750 m active fire products: Product user's guide version 1.4. Prod. User's Guid. Version 1, 23.
Schroeder, W., Giglio, L., Hall, J., 2024. Collection 2 visible infrared imaging radiometer suite (VIIRS) 375-m active fire product user's guide version 1.0.
Schroeder, W., Giglio, L., Hall, J., 2025. Collection 2 visible infrared imaging radiometer suite (VIIRS) 375-m active fire product user's guide version 1.2.
Schroeder, W., Oliva, P., Giglio, L., Csiszar, I.A., 2014. The new VIIRS 375 m active fire detection data product: Algorithm description and initial assessment. Remote Sens. Environ. 143, 85–96.
Sharples, J.J., 2009. An overview of mountain meteorological effects relevant to fire behaviour and bushfire risk. Int. J. Wildland Fire 18 (7), 737–754.
Siegert, F., Hoffmann, A.A., 2000. The 1998 forest fires in east kalimantan (Indonesia): A quantitative evaluation using high resolution, multitemporal ERS-2 SAR images and NOAA-AVHRR hotspot data. Remote Sens. Environ. 72 (1), 64–77.
Swaine, M., 1992. Characteristics of dry forest in West Africa and the influence of fire. J. Veg. Sci. 3 (3), 365–374.
Tang, X., Bullock, E.L., Olofsson, P., Woodcock, C.E., 2020. Can VIIRS continue the legacy of MODIS for near real-time monitoring of tropical forest disturbance? Remote Sens. Environ. 249, 112024.

Tedim, F., Leone, V., Amraoui, M., Bouillon, C., Coughlan, M.R., Delogu, G.M., Fernandes, P.M., Ferreira, C., McCaffrey, S., McGee, T.K., et al., 2018. Defining extreme wildfire events: Difficulties, challenges, and impacts. Fire 1 (1), 9.

Touge, Y., Shi, K., Nishino, T., Sun, C., Sekizawa, A., 2024. Spatial-temporal characteristics of more than 50,000 wildfires in Japan from 1995 to 2020. Fire Saf. J. 142, 104025.

Tymstra, C., Stocks, B.J., Cai, X., Flannigan, M.D., 2020. Wildfire management in Canada: Review, challenges and opportunities. Prog. Disaster Sci. 5, 100045.

Vadrevu, K.P., Ellicott, E., Badarinath, K., Vermote, E., 2011. MODIS derived fire characteristics and aerosol optical depth variations during the agricultural residue burning season, north India. Environ. Pollut. 159 (6), 1560–1569.

Val-Aguasca, J.P., Videgain-Marco, M., Martín-Ramos, P., Vidal-Cortés, M., Boné-Garasa, A., García-Ramos, F.J., 2019. Fire risks associated with combine harvesters: analysis of machinery critical points. Agronomy 9 (12), 877.

Valencia, A., Melnik, K.O., Kelly, R.J., Jerram, T.C., Wallace, H., Aguilar-Arguello, S., Katurji, M., Pearce, H.G., Gross, S., Strand, T., 2023. Mapping fireline intensity and flame height of prescribed gorse wildland fires. Fire Saf. J. 140, 103862.

Veraverbeke, S., Rogers, B.M., Goulden, M.L., Jandt, R.R., Miller, C.E., Wiggins, E.B., Randerson, J.T., 2017. Lightning as a major driver of recent large fire years in North American boreal forests. Nat. Clim. Chang. 7 (7), 529–534.

Wang, Z., Li, X., Zha, M., Ji, J., 2024. Experimental and numerical study on data-driven prediction for wildfire spread incorporating adaptive observation error adjustment. Fire Saf. J. 148, 104230.

Westerling, A.L., Hidalgo, H.G., Cayan, D.R., Swetnam, T.W., 2006. Warming and earlier spring increase western US forest wildfire activity. Science 313 (5789), 940–943.

Whittaker, R.H., 1970. Communities and ecosystems..

Wickramasinghe, C., Wallace, L., Reinke, K., Jones, S., 2020. Intercomparison of himawari-8 AHI-FSA with MODIS and VIIRS active fire products. Int. J. Digit. Earth.

Xu, G., Zhong, X., 2017. Real-time wildfire detection and tracking in Australia using geostationary satellite: Himawari-8. Remote. Sens. Lett. 8 (11), 1052–1061.

Zhang, Q., Dong, Y., Zheng, Y., Yu, H., Song, M., Zhang, L., Yuan, Q., 2024a. Three-dimension spatial–spectral attention transformer for hyperspectral image denoising. IEEE Trans. Geosci. Remote Sens. 62, 1–13.

Zhang, Q., Yuan, Q., Jin, T., Song, M., Sun, F., 2022a. SGD-SM 2.0: an improved seamless global daily soil moisture long-term dataset from 2002 to 2022. Earth Syst. Sci. Data 14 (10), 4473–4488.

Zhang, Q., Yuan, Q., Li, J., Li, Z., Shen, H., Zhang, L., 2020. Thick cloud and cloud shadow removal in multitemporal imagery using progressively spatio-temporal patch group deep learning. ISPRS J. Photogramm. Remote Sens. 162, 148–160.

Zhang, Q., Yuan, Q., Song, M., Yu, H., Zhang, L., 2022b. Cooperated spectral low-rankness prior and deep spatial prior for HSI unsupervised denoising. IEEE Trans. Image Process. 31, 6356–6368.

Zhang, Q., Zheng, Y., Yuan, Q., Song, M., Yu, H., Xiao, Y., 2024b. Hyperspectral image denoising: From model-driven, data-driven, to model-data-driven. IEEE Trans. Neural Netw. Learn. Syst. 35 (10), 13143–13163.

Zhang, Q., Zhu, J., Dong, Y., Zhao, E., Song, M., Yuan, Q., 2025. 10-Minute forest early wildfire detection: Fusing multi-type and multi-source information via recursive transformer. Neurocomputing 616, 128963.

Zhang, Q., Zhu, J., Huang, Y., Yuan, Q., Zhang, L., 2023. Beyond being wise after the event: Combining spatial, temporal and spectral information for Himawari-8 early-stage wildfire detection. Int. J. Appl. Earth Obs. Geoinf. 124, 103506.

Zhao, A., Chen, K., Guo, S., 2014. Estimation LAI of montane evergreen broad-leaved forest in southwest Sichuan using different spatial prediction models. J. Nat. Resour. 29 (4), 598–609.

Zheng, Z., Yang, W., Zhou, G., Wang, X., 2012. Analysis of land use and cover change in Sichuan province, China. J. Appl. Remote. Sens. 6 (1), 063587–063587.